AGU PUBLICATIONS

Water Resources Research

RESEARCH ARTICLE
10.1002/2016WR019742

Key Points:
- Soil stratigraphy allows for development of perched water tables, which activate depending on catchment storage state
- Spatial sources and dominant processes of runoff generation shift seasonally
- Shallow flow paths are necessary for substantial runoff and control active surface drainage length

Supporting Information:
- Supporting Information S1
- Figure S1

Correspondence to:
M. A. Zimmer,
margaret.zimmer@ucsc.edu

Citation:
Zimmer, M. A. and B. L. McGlynn (2017), Ephemeral and intermittent runoff generation processes in a low relief, highly weathered catchment, *Water Resour. Res.*, *53*, doi:10.1002/2016WR019742.

Received 1 SEP 2016
Accepted 25 APR 2017
Accepted article online 2 MAY 2017

© 2017. American Geophysical Union. All Rights Reserved.

Ephemeral and intermittent runoff generation processes in a low relief, highly weathered catchment

Margaret A. Zimmer[1,2] and Brian L. McGlynn[1]

[1]Earth and Ocean Sciences Division, Duke University, Durham, North Carolina, USA, [2]Now at Department of Earth and Planetary Sciences, University of California - Santa Cruz, Santa Cruz, California, USA

Abstract Most field-based approaches that address runoff generation questions have been conducted in steep landscapes with shallow soils. Runoff generation processes in low relief landscapes with deep soils remain less understood. We addressed this by characterizing dominant runoff generating flow paths by monitoring the timing and magnitude of precipitation, runoff, shallow soil moisture, and shallow and deep groundwater dynamics in a 3.3 ha ephemeral-to-intermittent drainage network in the Piedmont region of North Carolina, USA. This Piedmont region is gently sloped with highly weathered soils characterized by shallow impeding layers due to decreases in saturated hydraulic conductivity with depth. Our results indicated two dominant catchment storage states driven by seasonal evapotranspiration. Within these states, distinct flow paths were activated, resulting in divergent hydrograph recessions. Groundwater dynamics during precipitation events with different input characteristics and contrasting storage states showed distinct shallow and deep groundwater flow path behavior could produce similar runoff magnitudes. During an event with low antecedent storage, activation of a shallow, perched, transient water table dominated runoff production. During an event with high antecedent storage, the deeper water table activated shallow flow paths by rising into the shallow transmissive soil horizons. Despite these differing processes, the relationship between active surface drainage length (ASDL) and runoff was consistent. Hysteretic behavior between ASDL and runoff suggested that while seasonal ASDLs can be predicted based on runoff, the mechanisms and source areas producing flow can be highly variable and not easily estimated from runoff alone. These processes and flow paths have significant implications for stream chemistry across seasons and storage states.

1. Introduction

Much of catchment hydrology over the last several decades has focused on deciphering the components of runoff in small catchments [*Horton*, 1933; *Hewlett and Hibbert*, 1963; *Betson*, 1964]. Researchers have shown that runoff can be composed of fluctuating combinations of base flow and stormflow contributions depending on antecedent catchment storage state [*Pearce et al*., 1986; *Sklash et al*., 1986]. Stormflow contributions were often shown to be composed of shallow subsurface stormflow [*Tsukamoto*, 1963; *Weyman*, 1970], saturation-excess overland flow [*Dunne and Black*, 1970], and infiltration-excess overland flow [*Horton*, 1933]. These stormflow contributions were typically couched within the variable source area conceptual model [*Hursh*, 1936; *Hewlett and Hibbert*, 1966], which often focuses on the lateral expansion of source areas in response to precipitation inputs. While most studies invoked these processes to explain the stormflow component of runoff at a catchment outlet, few have linked these processes to the longitudinal expansion of the surface drainage network [in the sense of *Day*, 1983].

Surface flows expand and contract beyond their perennial waterways in response to precipitation events [*Day*, 1983] and fluctuating seasonal catchment storage states [*Godsey and Kirchner*, 2014; *Whiting and Godsey*, 2016]. Historically, researchers have focused their attention on capturing the dynamic nature of stream networks [*Roberts and Archibold*, 1978; *Blyth and Rodda*, 1973; *Roberts and Klingeman*, 1972; *Spence and Mengistu*, 2016], but only recently have researchers focused on explaining the mechanisms behind it [*Biswal and Marani*, 2010; *Godsey and Kirchner*, 2014; *Shaw*, 2015]. Although this surface drainage expansion and contraction behavior is globally ubiquitous, there is still a wide gap in our understanding of how, why, and where streams expand and contract across landscapes.

The longitudinally dynamic portions of surface drainage are typically classified by ephemeral and intermittent streams. In this study, ephemeral streams are defined as portions of the drainage network that activate

in direction response to precipitation events. Intermittent streams are defined as reaches with persistent runoff of 3 month duration or longer, which is activated by the seasonal rise in the water table. There is minimal consensus for the major drivers of activation or dry down of nonperennial reaches that lead to surface drainage expansion and contraction. *Biswal and Marani* [2010] argued that the contraction of a stream network could be represented by a geomorphological recession flow model, where the spatially constant drainage of an unconfined aquifer could explain stream length recession. In contrast, *Shaw* [2015] compared runoff recession characteristics to field mapped stream network contraction and concluded that network contraction did not directly control hydrograph recession rates. *Godsey and Kirchner* [2014] presented field collected data which highlighted discontinuities in runoff across the stream network, suggestive that the persistence of longitudinal flow was from an imbalance between geomorphology/transmissivity of the subsurface and the discharge contributions to the stream. *Godsey and Kirchner* [2014] effectively argued that the stream network longitudinally varied between a gaining and losing system depending locally on the aforementioned characteristics. More field validations of surface drainage network lengths together with runoff generation process investigations across different catchment storage states, landscapes, and climates are imperative to test these contradicting models.

The majority of our understanding of runoff contributions from hillslopes is based on studies conducted in steep landscapes with thin soils [*Burt and McDonnell*, 2015]. This makes it difficult to compare and contrast runoff generation processes across landscapes with different geomorphology. In steep systems, the redistribution of water across the landscape has been shown to be predominantly driven by topography [*Montgomery and Dietrich*, 1988; *Jencso et al*., 2009, *Detty and McGuire*, 2010; *Jencso and McGlynn*, 2011] and hillslope contributions depend on a storage state-driven connectivity between the more responsive riparian zones and the less hydrologically active upper hillslopes [*McGlynn and McDonnell*, 2003; *Ocampo et al*., 2006; *Jencso et al*., 2009, 2010].

In contrast, *Devito et al*. [2005] argued that the slope of the land surface is not necessarily the main control on hydrologic response in low relief landscapes. In fact, researchers have shown hydrologic response in hillslopes has been linked to soil characteristics [*Sidle et al*., 2000; *Buttle and McDonald*, 2002; *Gannon et al*., 2014] and soil confining layers due to contrasting hydraulic conductivities across horizons [e.g., *Weyman*, 1973; *Elsenbeer*, 2001; *Tromp-van Meerveld and McDonnell*, 2006; *Du et al*., 2016]. The layers with contrasting hydraulic conductivities that can lead to perched water tables, include, but are not limited to, the O/A horizon interfaces [*Ragan*, 1968; *Betson and Marius*, 1969], B to B/C soil horizon interfaces [*Weyman*, 1973], fragipans [*McDaniel et al*., 2008], glacial till [*Rodhe and Seibert*, 2011], and the underlying bedrock [*Woods and Rowe*, 1996; *Burns and McDonnell*, 1998; *Tromp-van Meerveld and McDonnell*, 2006]. In fact, there is a substantial body of literature focused on water table development in duplex soils, or a diagnostic soil type with texture contrasts between the A and B horizons [*Chittleborough*, 1992]. Specific to highly weathered soils, *Elsenbeer* [2001] advanced the concept of hydrologic end members in tropical landscapes, by categorizing soil types by whether or not they promote shallow flow path partitioning. While researchers have utilized this conceptual water source partitioning to connect internal catchment dynamics to physical and chemical stream characteristics in tropical landscapes [e.g., *Kinner and Stallard*, 2004; *Johnson et al*., 2006; *Crespo et al*., 2011], few studies include direct observations of internal processes or connect flow paths to network dynamics.

While topography has been shown to override the influence of soil horizonation [*Hammermeister et al*., 1982], soil stratigraphy can play an important role in the redistribution of water in low relief landscapes [*ven Chow*, 1964; *Weyman*, 1973; *Cox and McFarlane*, 1995]. For example, in arid South Australia, almost 90% of total subsurface flow was shown to occur as shallow subsurface lateral flow [*Hardie et al*., 2012]. That said, *Smettem et al*. [1991] and *Brouwer and Fitzpatrick* [2002] have shown that macropores distributed within the soil matrix allowed for bypass flow to occur, which prevented subsurface lateral flow path development at the A/B horizon interface. And while many of these disparate studies have quantified the nuances of flow paths along individual hillslopes, few studies have linked these findings to catchment outflow or stream network scale dynamics.

The soil-bedrock interface in steep, forested landscapes with humid climates has been shown to be an important impeding layer to fuel runoff generation [*Woods and Rowe*, 1996; *Brammer and McDonnell*, 1996; *Tromp-van Meerveld and McDonnell*, 2006; *van Verseveld et al*., 2008; *Graham et al*., 2010]. The mechanisms driving these lateral subsurface flow paths at the soil-bedrock interface have been likened as well as contrasted to the mechanisms driving lateral flow paths at the ground surface and in the shallow subsurface [*Hardie et al*., 2012; *Ameli et al*., 2015]. While this may be an important impeding layer in landscapes with shallow soils, recent work by *St*

Clair et al. [2015] has shown that bedrock topography can be substantially different from surface topography, especially in landscapes with deep soils. Further, in a landscape with highly weathered soils, the soil-bedrock boundary is separated by sometimes meters of saprolite, or highly weathered bedrock. Therefore, in these landscapes, the sharp boundary or rapid change in saturated hydraulic conductivity between weathered and unweathered material can be indistinct and may not serve as a platform for lateral subsurface flow to accumulate. In fact, *Tromp-van Meerveld and Weiler* [2008] suggested that the assumption in field-based and model-based studies that bedrock is impermeable to vertical flow has potentially slowed scientific progress in catchment hydrology over the last several decades. As a result, more work is required to compare and contrast shallow and deep subsurface flow path activation in landscapes with highly weathered, deep soils.

Further still, the storage state of a catchment, which is often defined as the wetness of a catchment as measured by soil moisture or groundwater levels, has been shown to not only impact runoff response [*Western et al*., 1999; *Penna et al*., 2011] but also impact preferential flow paths [*Sidle et al*., 2000], lateral subsurface flow paths on impeding layers [*Hardie et al*., 2012], and recession event characteristics [*Shaw et al*., 2013]. Researchers have shown threshold responses in runoff with increasing catchment storage states [e.g., *Western and Grayson*, 1998]. *Sidle et al*. [1995] showed that a zero-order hollow, which was inactive during dry conditions, became a significant contributor to runoff at a high enough catchment storage state threshold. *Detty and McGuire* [2010] showed a threshold response in runoff with increasing antecedent catchment storage and precipitation. They attributed a linear response above this threshold to the activation of preferential flow paths and utilization of more transmissive upper soil horizons with a rise in groundwater levels. *Grayson et al*. [1997] showed spatial patterns of shallow soil moisture displayed either a wet or dry state, with a minimal transitional period between the two states. In their study, lateral water movement along surface and subsurface flow paths dominated the distribution of water in the landscape during wet periods, whereas vertical water movement dominated during dry periods. Their study was conducted in a temperate landscape where the hydraulic conductivity of the soil profile decreased sharply with depth and a seasonal imbalance between precipitation and evapotranspiration was extensive. Although soil depths were less than 2 m at their study site, these are otherwise generally similar soil and climatic characteristics to the Piedmont region, USA and other low relief landscapes across the globe. It is unknown, however, if similar separation between vertical and lateral subsurface flow path characteristics can be drawn from seasonal changes in catchment storage state in other landscapes, such as the humid Piedmont region in the southeastern U.S. More research is needed to understand the role of catchment storage state on the activation of subsurface flow paths in shallow and deep portions of the soil system.

In this study, we built on the work by *Zimmer and McGlynn* [2017a] and *Zimmer and McGlynn* [2017b] who found that stream-groundwater head gradients in an ephemeral-to-intermittent drainage network at the Duke Forest Research Watershed (North Carolina, USA) were bidirectional dependent on catchment storage state. They found that when catchment storage was high, stream-groundwater head gradients were toward the stream and when catchment storage was low, stream-groundwater head gradients were away from the stream. A shallow, transient, perched water table was hypothesized to be the dominant runoff generation process when deeper groundwater gradients were away from the stream and runoff was hypothesized to be a significant source of groundwater recharge on an annual basis. Here we investigated the process drivers of active surface drainage length and runoff during different catchment storage states and stream-groundwater head gradients. We investigated how soil structure and stratigraphy across this low relief landscape coupled with regional climatic forcings could drive the hydrology of the catchment. Specifically, we addressed the following questions:

1. How does the stratigraphy and depth of soils in low relief landscapes influence water flow paths and runoff source areas?
2. What are the relative roles of a seasonally present, deep water table and shallow, transient, perched water tables in runoff generation?

2. Methods and Site Description

2.1. Study Site

This study was conducted in a 3.3 ha catchment within the Duke Forest Research Watershed in the Piedmont region of North Carolina, USA (Figure 1). This site is a satellite site to the Calhoun Critical Zone

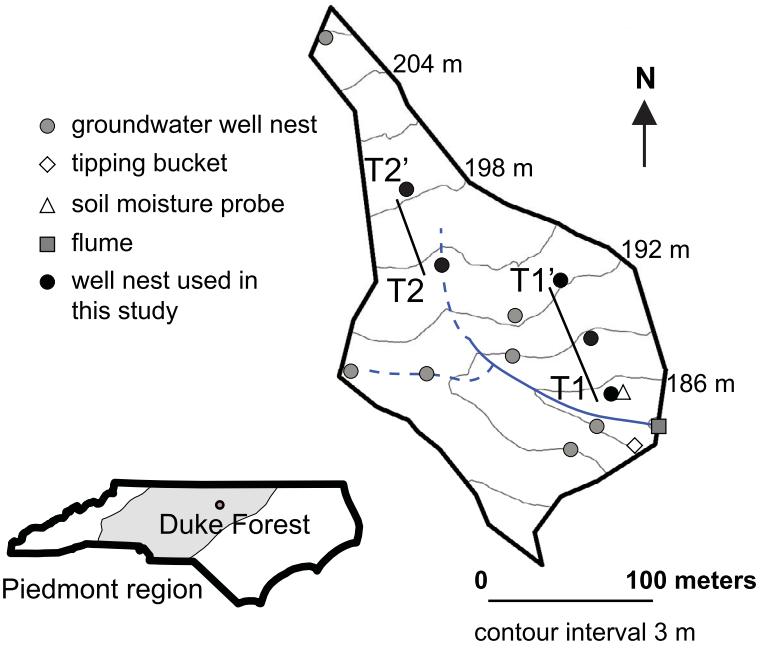

Figure 1. Instrumentation map of 3.3 ha research catchment, with bottom inset map indicating location of Duke Forest in North Carolina, USA, with shaded area indicating Piedmont physiographic region. Blue dashed lines indicate observed maximum extent of ephemeral streamflow and blue solid line indicates observed maximum extent of intermittent streamflow. Groundwater transects used in this study labeled as T1–T1′ (convergent hillslope) and T2–T2′ (zero order hollow).

Observatory located in the Piedmont region of South Carolina, USA. The catchment drains an ephemeral-to-intermittent drainage network and the gently sloped terrain ranges in elevation from 182 to 208 m. Duke Forest is characterized by a subtropical, humid climate with a mean annual temperature of 15.5°C, mean annual precipitation of 1136 mm yr^{-1}, and mean annual evapotranspiration of 720 mm yr^{-1} [*Novick et al.*, 2016]. Daily evapotranspiration was estimated from historic 30 min latent heat flux values collected from an eddy covariance flux tower located in the Duke Forest (Figure 2) [*Novick et al.*, 2016]. Four years (2003–2006) of the 8 year (2001–2008) latent heat flux collection period were used to calculate mean daily and annual evapotranspiration values presented in this study. These years were selected because they exhibited climatic and meteorological conditions most similar to the study period (e.g., removed drought years see Supplementral Information S1). The climate regime is almost entirely rain dominated with no seasonality in monthly precipitation (Figure 2) and a long growing season, typically from April to October (Figure 2). Forest communities present are characteristic of the region, with natural and planted pine (predominately loblolly pine, *Pinus taeda*) as well as many species of deciduous hardwoods, including oaks (*Quercus* spp.), hickories (*Carya* spp.), elms (*Ulmus* spp.), red maple (*Acer rubrum*), sweetgum (*Liquidambar styraciflua*), and tulip poplar (*Liriodendron tulipifera*). Forest age is approximately 80–100 years [*Oishi et al.*, 2008]. Historical land use activity included widespread agricultural practices, such as farming and tobacco production, which was common across the region and occurring predominantly in the eighteenth through early twentieth centuries [*Richter et al.*, 1999].

2.2. Subsurface Characteristics

The catchment is located within the Carolina Slate Terrane, which is composed of fine-grained felsic, metamorphic rock [*Bradley and Gay*, 2005], overlain by Ultisol soils of the Georgeville silt loam series [*Soil Survey Staff Natural Resources Conservation Service, United States Department of Agriculture*, 2016]. Based on hand-augered installation of 12 wells to refusal depths across the catchment (Figure 1), soil depth is characterized as nonuniform, with shallow soils in lower hillslopes (∼1 m) and deeper soils in upper hillslopes (>9 m; Figure 3). Increasing soil depth away from the stream (e.g., Figure 3) is suggestive of a bedrock topography that does not follow surface topography and is instead relatively horizontal. Similar observations of weathered and unweathered bedrock topography were confirmed by geophysical techniques at the nearby Calhoun Critical Zone Observatory [*St Clair et al.*, 2015].

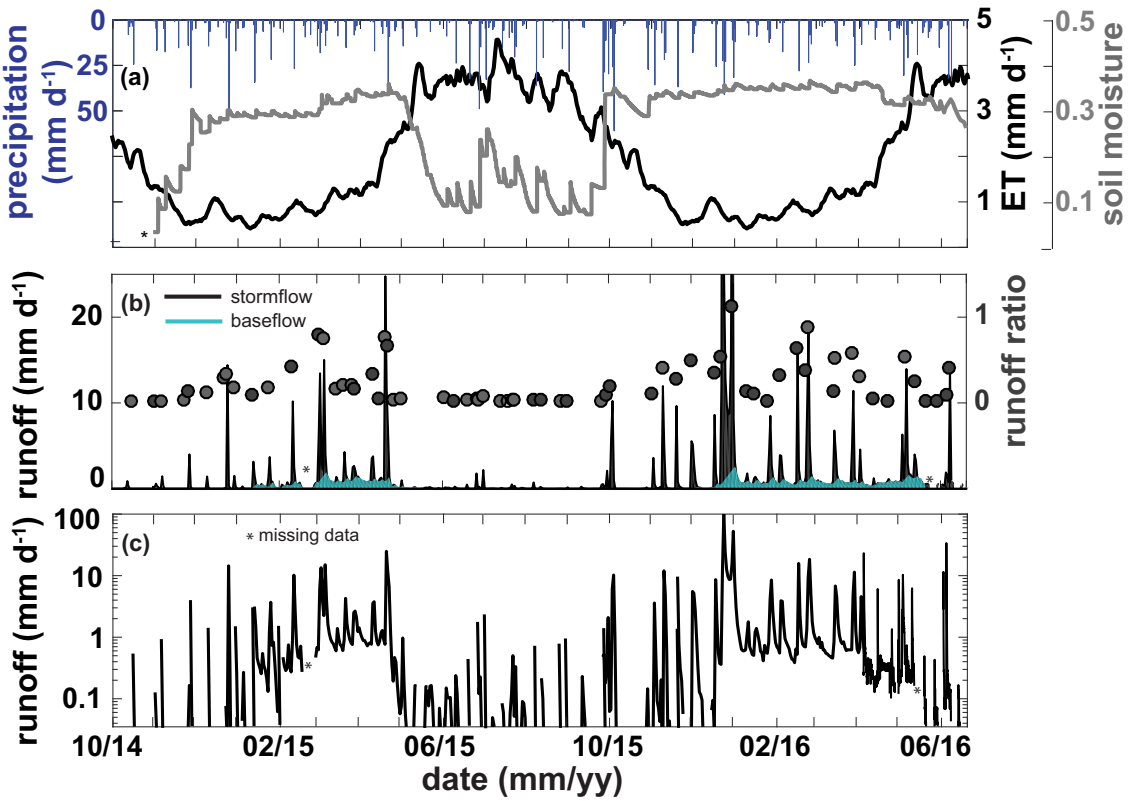

Figure 2. (a) Daily precipitation (blue bars), 3 day minimum volumetric water content (grey line) in the A horizon of a lower hillslope (T1), and daily evapotranspiration (black line) as adapted from *Novick et al*. [2016]. (b) Runoff ratios (grey circles) with time series of runoff separated into base flow (light blue) and stormflow (black) components (methods adapted from *Hewlett and Hibbert* [1963]). (c) Runoff in semilog scale to highlight seasonality in flow dynamics.

Vertical profiles of field-saturated hydraulic conductivity (K_{sat}; Figure 4 and Table 1) were characterized through different methods for saturated and unsaturated soil conditions. A compact constant head permeameter (K_{sat}, Inc., North Carolina, USA) [*Amoozegar*, 1989] and Glover's analytical solution [*Elrick and Reynolds*, 1992] were used to calculate K_{sat} at 15 cm depth intervals in unsaturated soil conditions. In saturated conditions, bail tests in groundwater wells [*Bouwer and Rice*, 1976] were used to calculate an integrated K_{sat} measurement across the screened interval where the water table was present (Figure 4 and Table 1). These variable depth K_{sat} measurements were taken at one lower hillslope site and at one upper hillslope site coincident with the groundwater well nest transect T1–T1′ (Figures 1 and 3). These measurements showed contrasting K_{sat} between the A and Bt horizons and the Bt and C horizons (Table 1 and Figure 4). This is in

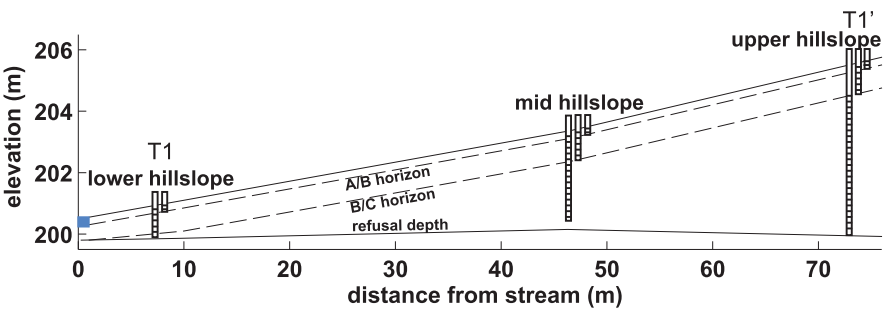

Figure 3. Cross section of T1–T1′, a groundwater well transect located along a characteristic convergent hillslope at the study site. Blue rectangle designates stream location at base of hill. Dashed lines represent breaks in field-measured saturated hydraulic conductivity (see Table 1), coincident with soil horizon interfaces and well installation depths. Refusal depth indicates depth of deepest well or piezometer (piezometers not shown) at each nest. Each well is shown to depth of installation with screen interval represented by horizontal lines along well length.

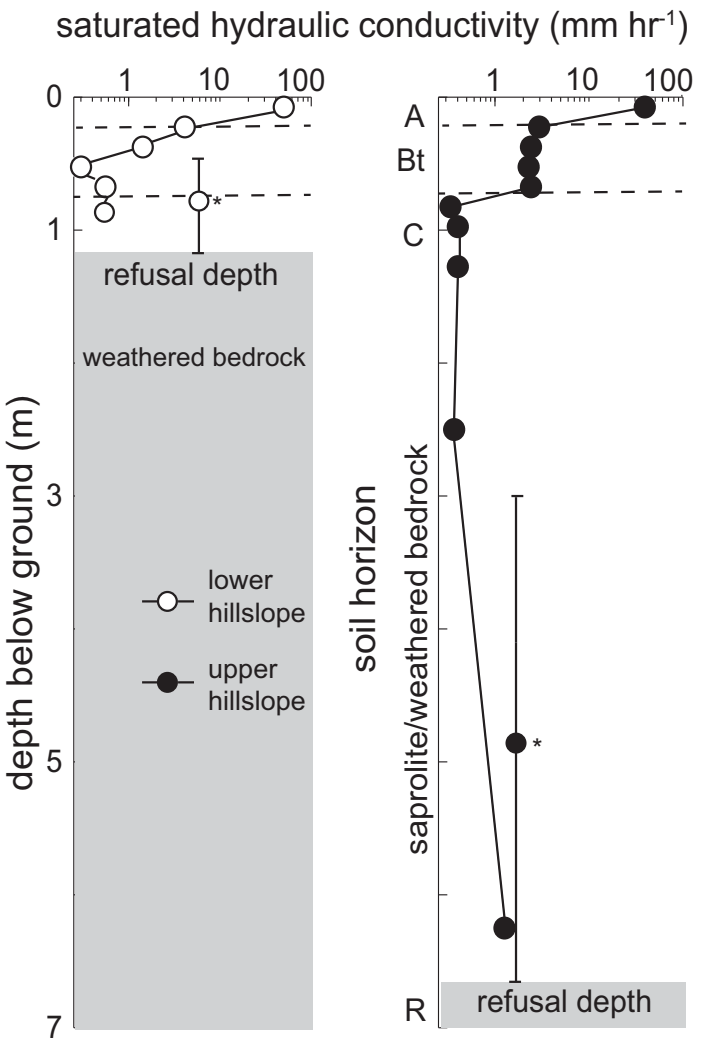

Figure 4. Field-measured saturated hydraulic conductivity (mm/h) measured using a constant head permeameter at distinct depths (centered within 15 cm measurement intervals) in a representative lower hillslope (T1) and upper hillslope (T1′) soil column. Grey boxes represent weathered bedrock below refusal depth. Asterisks represent average saturated hydraulic conductivity measurements from bail tests in wells co-located at permeameter measurement sites.

agreement with the soil series description by the *Soil Survey Staff Natural Resources Conservation Service, United States Department of Agriculture* [2016], which defined the local Georgeville soil series to have multiple argillic Bt horizons. For example, at the upper hillslope site (T1′), K_{sat} shifted from 29.3 mm h^{-1} in the A horizon to an average 2.4 mm h^{-1} across the Bt horizons (Table 1). This break in K_{sat} has been shown to limit the majority of the rooting zone to the upper 35 cm [*Oren et al*., 1998]. Within the Bt soil horizons, K_{sat} decreased with depth, reaching a profile minimum in the lower Bt horizon of 0.2 mm h^{-1} (Figure 4 and Table 2). Within the C horizon/saprolite layer, K_{sat} increased slightly from the lower Bt horizon. Similar breaks in K_{sat} coincident with soil horizon interfaces were seen in the lower hillslope measurement site (T1), although the refusal depth for sampling and well installation was just below the Bt/C horizon interface (Figure 4 and Table 1). Constant head double ring infiltrometer (Soilmoisture Equipment Corp., California, USA) experiments [*Johnson*, 1963] yielded infiltration rates that exceeded precipitation intensities measured during the study period.

2.3. Physical Hydrology

2.3.1. Active Surface Drainage Length Surveys

Active surface drainage length (ASDL) was recorded during 77 surface drainage network mapping campaigns over a wide range of runoff magnitudes (Figures 5 and 6). Surveys were conducted seasonally, represented by circles in Figure 5, as well as in high resolution snapshots across the rising and receding limbs of stormflow hydrographs, as represented by triangles and diamonds in Figure 5. Each surface drainage network inventory included a width measurement of the visible flow and a depth measurement in the thalweg at defined locations every 10 m along the network, from the catchment outlet to the farthest upstream presence of surface flow. This included flow within the geomorphic channel extent, which was characterized by an incised channel with banks and a definable channel head, as well as any observed overland flow beyond the geomorphic channel head. The geomorphic channel network length was 124 m and consisted of one unbranched channel. Overland flow beyond the channel originated at the channel head as well as at the beginning of a zero order hollow that intersected the main channel roughly 110 m upstream of the catchment outlet (Figure 1). These ephemeral surface flow paths showed presence of displaced leaves and debris, but with only minor sediment

Table 1. Clay Content (%) and Saturated Hydraulic Conductivity (K_{sat}, mm/h) for Select Soil Depth Intervals in the Soil Profile of a Characteristic Lower Hillslope (T1) and Upper Hillslope (T1′; see Figure 1 for Site Location)[a]

Depth Interval (m)	Approximate Soil Horizon Depth	Lower Hillslope		Upper Hillslope	
		Clay Content (%)	K_{sat} (mm/h)	Clay Content (%)	K_{sat} (mm/h)
0–0.15	A	5	47.5	15	29.3
0.15–0.30	A/Bt	13	4.2	21	4.4
0.30–0.45		14	1.5	42	1.8
0.45–0.60		14	0.2	43	1.7
0.60–0.75	Bt	14	0.5	41	1.8
0.75–0.90		8	0.6	40	0.2
0.90–1.05		4	5.5*	39	0.3
1.05–1.50	C		Refusal depth	34	0.3
1.50–2.00				20	
2.00–3.00				25	0.4
3.00–4.00	Saprolite/weathered bedrock			27	
4.00–5.00				16	1.9*
5.00–6.00				18	
6.00–7.00				21	1.2

[a]Depth to refusal was indicative of the upper bedrock weathering front. All K_{sat} measurements were from a constant head permeameter, except those designated with an asterisk, which were measured from bail tests. See Figure 4 for vertical range of subsurface covered in bail tests.

displacement and no discernable channel head. Within each 10 m survey interval, the degree of stream connectedness was recorded, i.e., how many meters of the 10 m survey length had surface flow (0–10 m scale). For each 10 m section, if the degree of stream connectedness was greater than 5 m, that section was categorized as fully connected, as macropores and other subterranean features often connected surface flow over short distances. For each surface drainage network inventory, the total active surface drainage length was calculated by summing each consecutive 10 m section length with flowing stream water (Figure 5).

2.3.2. Precipitation and Runoff Measurements

Precipitation and throughfall at 5 min intervals were recorded using 0.1 mm increment tipping buckets (Campbell Scientific, USA). Throughfall was recorded near the catchment outlet (Figure 1), while direct precipitation was recorded in a forest clearing 200 m outside the catchment (not pictured in Figure 1). Due to a small spatial area, with minimal potential for orographic effects and small spatial scale heterogeneity (e.g., small scale convective cells), precipitation was assumed uniform across the study catchment. As canopy interception causes throughfall to be spatially variable, the precipitation time series was used in this study. Stage level in the stilling well of a 0.9144 m (3 ft) H flume located at the catchment outlet was recorded every 5 min using a Tru Track Inc. (±1 mm resolution, New Zealand) capacitance water level recorder. Manual measurements of flume stage were conducted monthly using visual stage readings to corroborate capacitance rod measurements. Stage was converted to runoff using the conversion equation related to the specific flume geometry [*U.S. Department of Agriculture*, 1972] and confirmed with periodic instantaneous runoff measurements.

Table 2. Characteristics for Two Representative Precipitation Events Highlighted in This Study[a]

Event Characteristics	Event 1: March 2015 High Storage State	Event 2: October 2015 Low Storage State
Antecedent VWC (%)	30	13
Rainfall amount (mm)	19.8	86.6
Max hourly intensity (mm/h)	5.7	14.6
Max 5 min intensity (mm/5 min)	1.3	2.2
Stormflow (mm)	14.8	15.0
Runoff ratio	0.74	0.18
% exceedance (peak flow) Oct 2014 to Jun 2016	2.8	2.1

[a]Antecedent water content was defined as three day average prior to the event.

2.3.3. Groundwater Measurements

Groundwater dynamics were monitored at 5 min intervals in 12 nests of variable depth wells and piezometers using a combination of capacitance rods (Tru Track, New Zealand) and pressure transducers (±0.1 mm resolution, Solinst, USA). The well nests were distributed across a range of landscape positions, including lower hillslope, mid hillslope, and upper hillslope locations in valley hollows and convergent and planar hillslopes (Figure 1). At each nest, wells were installed to the A/Bt horizon interface (~25 cm depth, coincident with a sharp decrease in K_{sat}) and to a

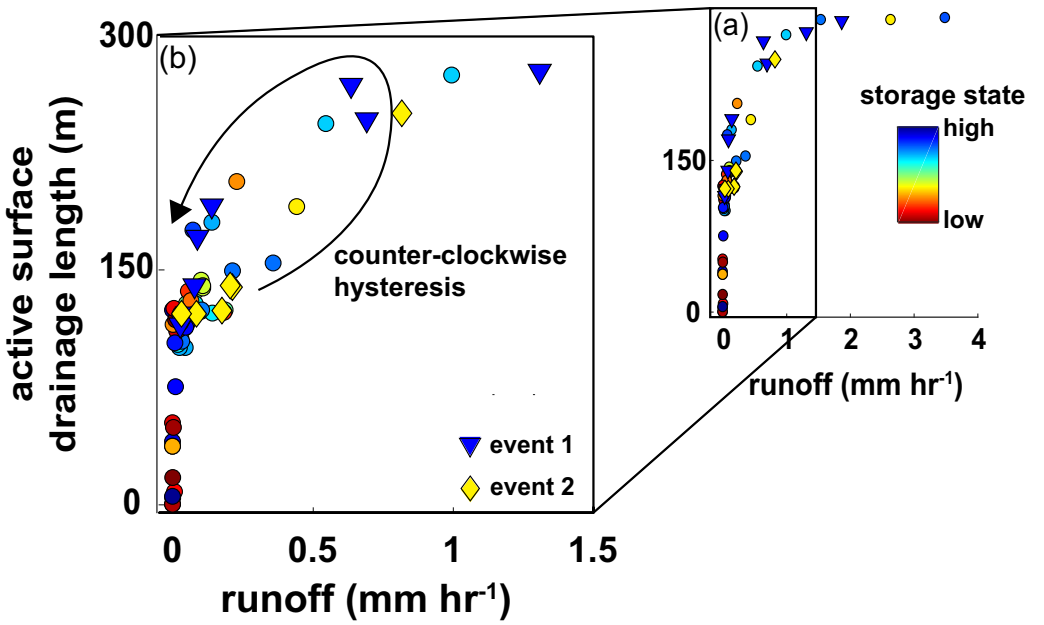

Figure 5. Measured active surface drainage length (ASDL) versus runoff at catchment outlet at time of ASDL measurement. (a) ASDL measurements for all 77 surface drainage mapping campaigns. (b) ASDL measurements across low and intermediate runoff values to highlight counterclockwise hysteresis in ASDL-runoff relationship. Color gradient represents storage state at time of measurement, calculated from daily evapotranspiration [*Novick et al.*, 2016]. Dark blue triangles represent surface drainage length surveys conducted during a precipitation event when catchment storage state was high (Event 1) and yellow diamonds represent surface drainage length surveys conducted during an event when catchment storage state was low (Event 2). Active surface drainage length values above 124 m represent surface flow beyond the geomorphic channel network.

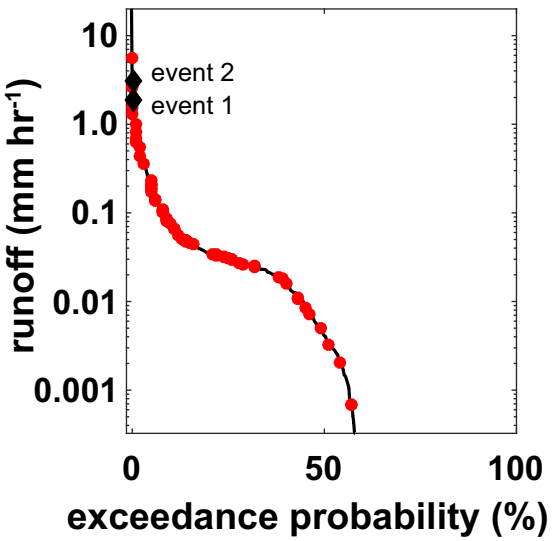

Figure 6. Exceedance probabilities for catchment outlet runoff across entire study period, 1 October 2014 through 20 June 2016. Exceedance probability above 58% indicates periods during the study when the stream at the catchment outlet was dry. Red circles represent flow conditions when active surface drainage length surveys were conducted. The two black diamonds represent the peak runoff for two precipitation events highlighted in this study and introduced in section 3.4 and described in Table 2.

refusal depth (upper bedrock weathering front, depth variable; Figure 3). Piezometers were coupled with the deepest well at each nest (Figure 3). All piezometers were solid PVC pipe open at the bottom, while wells were fully screened to within 10 cm of the ground surface. In locations where the refusal depth exceeded 3 m, intermediate wells were installed to ~1 m depth, which was approximately at the Bt/C horizon interface. In those locations, the deepest well was screened to 1 m of the ground surface to isolate the deeper groundwater signal from any shallow flow paths. Data reported in this study were collected from 1 October 2014 through June 2016, with specific focus on two precipitation events with contrasting catchment storage states. For simplicity, data from 5 of the 12 groundwater nests installed in the catchment were used in this study (highlighted in Figure 1). These nests captured shallow groundwater dynamics along transects installed in characteristic geomorphic landscape features, specifically a convergent hillslope (Transect T1; Figures 1 and 3) and a zero order hollow (Transect T2; Figure 1). The zero order hollow

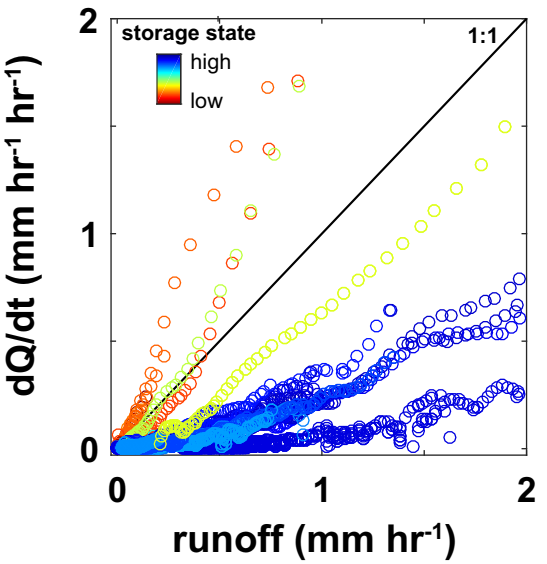

Figure 7. The change in runoff per the change in time versus instantaneous runoff across the stormflow hydrograph recessions of 32 precipitation events during the study period (section 2.3.4.3 for details on event selection). Color gradient represents the general catchment storage state during each event.

was characterized as a convergent hillslope with enough upslope area to accumulate surface drainage that could displace leaves and debris.

2.3.4. Hydrologic Metric Calculations

2.3.4.1. Catchment Storage State

Catchment storage state was defined as high, low, or transitional based on seasonal evapotranspiration, soil moisture, and runoff dynamics. Daily evapotranspiration was averaged from 4 years of data (2003–2006; see section 2.1) collected every 30 min from an eddy covariance flux tower located in the Duke Forest [*Novick et al.*, 2016]. At the lower hillslope zone of T1, a 12 cm soil water content reflectometer (Campbell Scientific, USA) was installed vertically from 5 to 17 cm depth below ground to capture shallow soil water content dynamics at 5 min intervals. Shallow soil water content was filtered to a 3 day antecedent minimum to represent generalized catchment storage state conditions (Figure 2). A relatively short window was used for calculating the representative shallow soil water content in order to correspond with the flashy nature of the system.

Soil moisture was high and runoff was seasonally persistent (i.e., intermittent flow) at the catchment outlet when evapotranspiration was low. This occurred approximately between midwinter and early summer each year and catchment storage state was classified as high (Figure 2). Soil moisture was low and runoff at the catchment outlet only occurred in direct response to precipitation (i.e., ephemeral flow) when evapotranspiration was high (Figure 2). This occurred early summer to midwinter and catchment storage state was classified as low. The transitional periods between high and low catchment storage states were minor and referred to the brief period when groundwater and stream levels dropped or rose between states (Figure 2). More details on these catchment storage state dynamics, including detailed discussion of resulting stream-groundwater head gradients, can be found in *Zimmer and McGlynn* [2017b].

2.3.4.2. Hydrograph Separation

Hydrograph separation of base flow and stormflow components was conducted for the period when catchment storage state was high and runoff was persistent (Figures 2 and 7). For the rest of the year, when storage state was low and runoff occurred solely in response to precipitation, any runoff that occurred was assumed to be entirely composed of stormflow. For the applicable time periods, methods presented by *Hewlett and Hibbert* [1966] were adapted to separate base flow from stormflow. Specifically, a linear increase (0.00012 mm h^{-1}) in base flow contributions was used for each 5 min time step during each hydrograph response to a precipitation event. For each precipitation event, the stormflow component ceased when base flow contributions intersected the hydrograph on the receding limb. All runoff between precipitation events was assumed to be composed entirely of base flow contributions.

2.3.4.3. Runoff Ratios and Recession Rates

Runoff ratios (stormflow/precipitation) were calculated for 75 precipitation events (>8 mm input with >12 h between precipitation events in order to accurately isolate individual stormflow hydrographs), where stormflow was represented by total runoff minus base flow (see section 2.3.4.2 for base flow calculations). Hydrograph recession rates were calculated for a subset of events following the methods outlined by *Brutsaert and Nieber* [1977]. Only events with no additional precipitation inputs after the peak of the storm hydrograph were used (32 events) so that recession rates were not impacted by new precipitation inputs. The period used for recession rate analysis for each event was from the hydrograph peak to the end of the stormflow hydrograph, either defined as when one or more of the following criterion were met: runoff ceased when base flow was not present, runoff decreased to 120% of prestorm magnitudes when base flow was present, or precipitation from the next event occurred. Of the 32 precipitation events used for this

analysis, 10 occurred when catchment storage state was low (no base flow), 17 when storage state was high (base flow was present), and 5 occurred in transitional periods. Transitional periods occurred when flow was not persistent (no or minimal base flow), but runoff was fed by the deeper groundwater system. This characteristic is described in further details in section 3.

3. Results

3.1. Active Surface Drainage Length

From 77 surface drainage mapping campaigns, measured active surface drainage length (ASDL) ranged between 0 when the stream channel was dry and 286 m at its observed maximum extent (Figure 5). Surveys occurred across a wide range of flow conditions, represented by flow exceedance probabilities from 0.07 to 58%, where percentages above 58 represented periods when runoff was nonexistent (Figure 6).

Runoff was positively correlated to ASDL ($r^2 = 0.81$, nonlinear regression in the form of an exponential rise to maximum). At the longer observed ASDLs (>280 m), a wide range of runoff values were recorded (Figure 5). The geomorphic channel network (defined in section 2.3.1) was 124 m long; ASDL measurements greater than 124 m generally represented ephemeral saturated overland flow beyond the geomorphic channel network. Some minor scatter in the relationship between ASDL and runoff occurred when runoff was between 0.1 and 1.0 mm h^{-1} and ASDL was between 124 and 268 m (Figure 5b). This scatter resulted from counterclockwise hysteretic behavior between ASDL and runoff across individual stormflow hydrographs. In two of the three high temporal resolution snapshots of ASDL during precipitation events, ASDL was higher on the receding limb than on the rising limb (e.g., triangles in Figure 5b). These two precipitation events occurred when catchment storage state was high. The other high temporal resolution snapshot mapping campaign that occurred during a precipitation event when catchment storage state was low showed no hysteretic behavior in the ASDL-runoff relationship (diamonds in Figure 5b).

3.2. Seasonal Catchment Storage, Soil Moisture, and Runoff Dynamics

With a lack of seasonality in monthly precipitation, changes in catchment storage state were largely driven by evapotranspiration (Figure 2). During the dormant season, approximately November–February, evapotranspiration rates were low, which allowed for soil moisture accumulation (Figure 2). During the growing season, approximately March–October, evapotranspiration rates were higher, which lowered soil moisture (Figure 2). This seasonality in evapotranspiration produced two dominating catchment storage states (high or low) with rapid transitional periods (Figure 2).

The evapotranspiration-controlled catchment storage state produced seasonality in runoff persistence, runoff ratios (Figure 2), and recession characteristics (Figure 7). Runoff at the catchment outlet was seasonally persistent (i.e., intermittent flow) from midwinter to late spring (Figure 2), when catchment storage state was high. During this period, any interstorm runoff was considered base flow, which composed 35 and 24% of total runoff during the 2014 and 2015 winters, respectively. During the rest of the year when catchment storage state was low, runoff at the catchment outlet was ephemeral and 100% of runoff was considered stormflow.

Runoff ratios from 75 precipitation events ranged from 0.08 to 1.2, with a strong seasonal pattern (Figure 2). Runoff ratios were generally low when catchment storage state was low and high when the storage state was high (Figure 2). Large ratios above 1 (more runoff than precipitation during an event) occurred due to several large successive precipitation events when catchment storage state was high. Hydrograph recession rates for a subset of 32 precipitation events were greater during events that occurred when catchment storage state was low when compared to events that occurred when storage state was transitional or high (Figure 7).

While recession characteristics and runoff ratios varied dependent on catchment storage state, similar stormflow magnitudes were produced from a wide range of precipitation amounts and intensities (Figure 8). Inversely, similar precipitation amounts produced a wide range in stormflow magnitudes. For example, the dashed lines across Figure 8 highlight several events that had similar precipitation amounts, but resulted in a wide range in runoff, or a wide range in precipitation with similar runoff magnitudes. Storm intensity across 5 min, 15 min, and hourly periods did not play an apparent role in controlling these

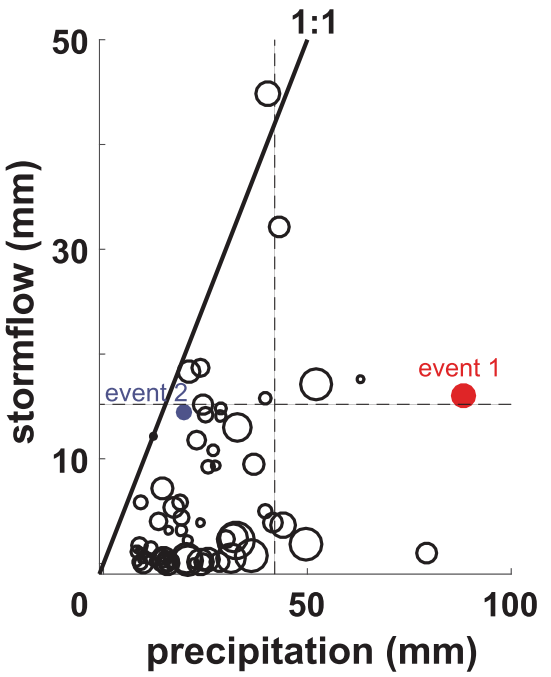

Figure 8. Total precipitation versus stormflow (total runoff-base flow) for 75 precipitation events that occurred during the study period. Circle sizes were scaled to the maximum hourly precipitation intensity for each event. The blue and red circles represent the precipitation Events 1 and 2, respectively, highlighted in this study. Horizontal dashed line highlights similar stormflow magnitudes for a wide range in precipitation amounts and vertical dashed line highlights similar precipitation totals for a wide range in runoff.

patterns and discrepancies, as shown by the variation in circle size in Figure 8, which represented maximum hourly precipitation intensity for each event.

3.3. Shallow and Deep Water Table Partitioning

3.3.1. Seasonally Persistent Water Table

The height of the water table was strongly controlled by evapotranspiration (Figures 2 and 9). Catchment storage state increased due to decreased evapotranspiration (Figure 9), which allowed recharge of precipitation and soil water to the water table. This was reflected in the seasonal rise in groundwater levels in the deep wells (dark lines in Figure 9). During periods when the water table was present in the hand-augered wells, runoff was persistent (Figure 2) and hillslope groundwater head gradients were toward the stream, as evident in Figure 9 and described by *Zimmer and McGlynn* [2017a] and *Zimmer and McGlynn* [2017b]

When evapotranspiration rates increased in late spring, the catchment storage state decreased (Figure 2), the seasonal water table in the deeper wells dropped (dark lines in Figure 9), and runoff at the outlet became ephemeral, in that runoff occurred only in direct response to precipitation (Figure 2). During this period, groundwater head gradients were away from the stream, as evident in Figure 9 and discussed in *Zimmer and McGlynn* [2017a] and *Zimmer and McGlynn* [2017b]. Once the seasonal water table dropped below the deepest wells in the mid and upper hillslope wells, it did not rise back into the wells until the start of the next dormant season, when evapotranspiration decreased again (dark lines in Figure 9). In the lower hillslope well nests, there was minimal groundwater response to precipitation inputs in the deeper well when catchment storage state was low (dark line in Figure 9).

3.3.2. Shallow, Transient, Perched Water Table

While the wells installed to refusal depths captured the seasonal rise and fall of the water table, wells in the intermediate and upper soil horizons captured shallow, transient, perched water table dynamics (Figure 9). These shallow flow paths activated in response to both increased seasonal catchment storage state and individual precipitation events (Figure 9). Due to strong contrasts in K_{sat} between soil horizons (Table 1 and Figure 4), evidence of a shallow, transient, perched water table occurred both at the A/Bt and Bt/C horizon interfaces (Figure 9). This perching behavior was seen in shallow wells at every landscape position, as demonstrated in the lower, mid, and upper hillslope well nests of T1–T1′ (Figure 9).

When catchment storage state was low and runoff at the catchment outlet only occurred in direct response to precipitation inputs (i.e., ephemeral runoff), the seasonal water table was below the bedrock weathering front and did not contribute to runoff (Figure 9). During that time, any groundwater seen in hillslopes was transient and perched at the A/Bt and Bt/C soil horizon interfaces in direct response to precipitation inputs (Figure 9). When catchment storage state was high, the deeper water table rose into the upper soil horizons at the lower and mid hillslope well nests. Due to this elevated water table, there was no perching of transient water tables in these landscape positions when catchment storage was high. Instead, groundwater was continuous with depth. In the upper hillslopes, however, the water table never rose above the saprolite and into the upper soil horizons where the shallow, transient, perched water tables were located. This produced consistently disconnected shallow and deep groundwater flow paths in the upper hillslopes, regardless of catchment storage state (Figure 9) [see *Zimmer and McGlynn*, 2017a for more details]. That said, the

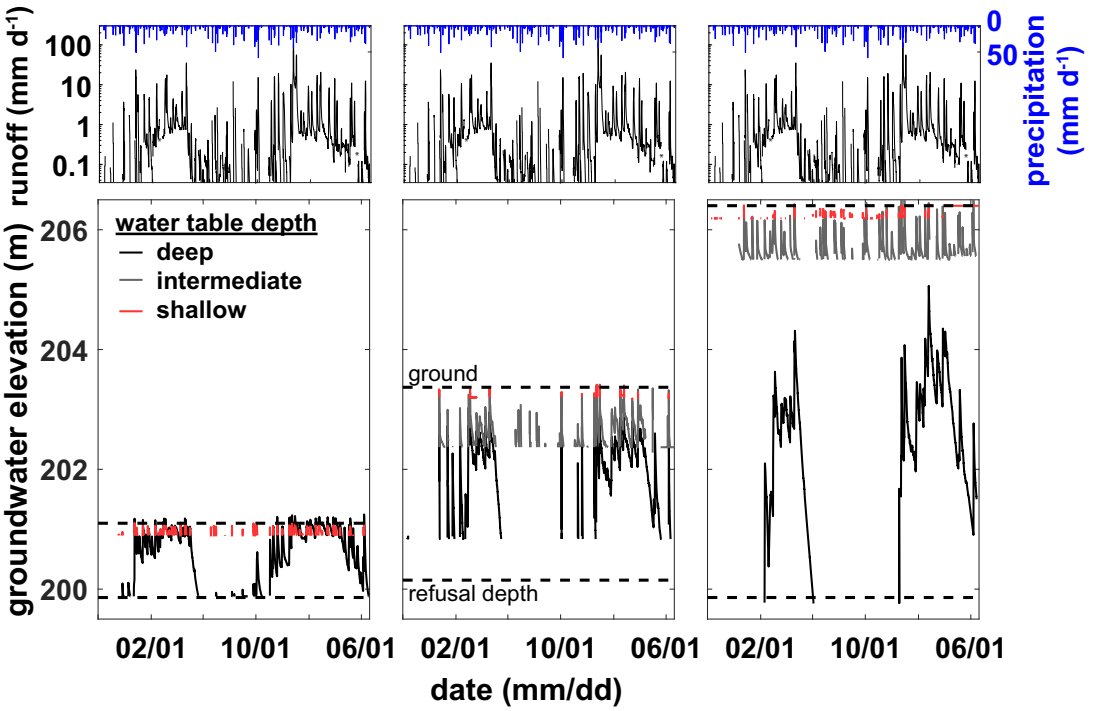

Figure 9. (top row) Time series of daily precipitation and runoff at catchment outlet. Runoff time series is shown in semilog space to highlight runoff seasonality. (bottom row) Time series of groundwater dynamics in shallow, intermediate, and deep wells across T1–T1′ transect. See Figure 1 for location in catchment and see Figure 3 for conceptual schematic of well installation locations and depths along transect. At the lower hillslope and mid hillslope sites, perched water tables in shallow and intermediate wells occurred when runoff was ephemeral. Shallow and deep water tables connected when runoff was persistent. At the upper hillslope site, shallow perched water tables were always disconnected from the deeper water table.

intermediate well installed to 1 m depth (∼Bt/C horizon interface) at the upper hillslope of T1′ showed a perched, seasonal water table (e.g., sustained interstorm saturation), not just a transient, storm-derived, perched water table as seen in wells installed to the A/Bt horizon in other landscape positions.

3.3.3. Runoff Response to Water Table Development

Results showed distinct differences in the relationships between runoff and the water levels of both the seasonally persistent, deep water table and the shallow, transient, perched water table. To highlight these differences, data from the groundwater levels in the deep and shallow wells at the upper hillslope well nest along the T1–T1′ transect are presented in Figure 10 (Figure 1 for location). In the deep well, which captured seasonal dynamics of the deeper water table, substantial runoff occurred with or without contributions from this deeper water table (Figure 10). Further, while the rise of this deeper water table was driven by catchment storage state, high runoff occurred at a range of catchment storage states and water levels (Figure 10). In contrast, in the shallow well, which captured the shallow, perched water table at the Bt/C horizon interface, presence of this water table was necessary for substantial runoff (Figure 10). This relationship was not necessarily driven by catchment storage state, as high water levels and runoff occurred across a range of storage states.

3.4. Runoff and Groundwater Dynamics in Contrasting Catchment Storage States

The next two sections describe the different shallow and deep groundwater dynamics that produced similar runoff magnitudes across two distinct precipitation events with contrasting catchment storage states. Event 1 was a midintensity precipitation event that occurred when catchment storage state was high and was characteristic of precipitation events that occur during the dormant season in the Piedmont, when evapotranspiration is low (Table 2). Event 2 was a higher intensity precipitation event that occurred when catchment storage state was low, representative of precipitation events that occur during the active growing season in the Piedmont, when evapotranspiration is high (Table 2).

3.4.1. Precipitation Event During a High Catchment Storage State

A precipitation event (Event 1) in March 2015 was intensively monitored when the deep water table was elevated, catchment storage was high, and base flow was present (Table 2). Precipitation intensity was

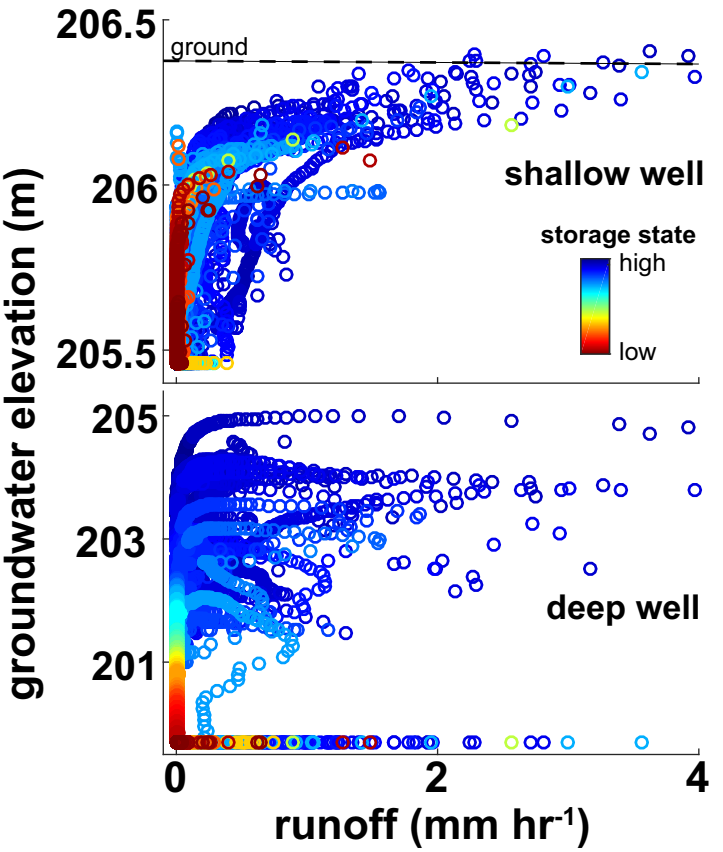

Figure 10. Runoff versus the groundwater elevation in the (top) shallow and (bottom) deep nested wells in an upper hillslope location (T1′; see Figure 1 for location). Color gradient represents storage state at time of measurement, calculated from daily evapotranspiration [*Novick et al.*, 2016].

relatively uniform across the event period (Figure 11 and Table 2). Prior to the event, runoff was present longitudinally across the entire geomorphic channel network for an active surface drainage length (ASDL) of 124 m. During the event, the ASDL expanded beyond the geomorphic channel network as saturated overland flow in 2 zero order hollows beyond the channel head to a maximum ASDL of 286 m. After stormflow ceased, the ASDL receded back to 124 m (Figures 5 and 11).

Prior to the precipitation event, the seasonal water table was elevated well into the upper soil horizons across the lower hillslopes (Figure 11). In the lower hillslope nests (T1 and T2), the water table was elevated into the zone of the shallow wells (~25 cm depth). As a result, there was no perched water table present at these locations during the precipitation event. In the upper hillslope groundwater (T1′ and T2′), the deeper water table was disconnected from the shallower water table (Figure 11). As a result, there were perched water tables in the upper hillslopes of the catchment before, during, and after the precipitation event.

At the lower hillslope well nest (T1), groundwater levels rose above the ground surface, which produced saturation-excess overland flow (Figure 11). The shallow flow paths at the upper hillslope well nests (T1′ and T2′) were at the soil surface, suggesting saturation-excess overland flow across upper hillslopes in the catchment may have occurred, although it was not observed in person. In all well nests, the initial groundwater response was simultaneous with the initial runoff response (Figure 11). Macropore flow was a potential driver of rapid groundwater response at depth, however macropore flow observations did not occur in this study. Overall, groundwater levels had a more subdued response to precipitation inputs than the stream hydrograph. In most wells, groundwater plateaued before the storm hydrograph peaked (Figure 11). In the lower hillslope well nests, groundwater levels receded to preevent levels within the time frame of the hydrograph recession. In the upper hillslope well nests, groundwater levels took up to 3 days to recede back to preevent levels (Figure 11).

3.4.2. Precipitation Event During a Low Catchment Storage State

An additional precipitation event (Event 2) was intensively monitored in October 2015, when the seasonal water table was below the deepest well depth, catchment storage was low, and base flow was not present (Table 2 and Figure 11). Storm intensity was variable throughout the event period, which resulted in several hydrograph peaks (Figure 11). Prior to the event, runoff was absent and the ASDL was 0 m. During the event, the ASDL expanded beyond the geomorphic channel as overland flow up the zero order hollows to an observed maximum length of 265 m (Figures 5 and 11).

Before the precipitation event, groundwater was absent in all wells except the intermediate well (installation to ~Bt/C horizon) in the upper hillslope nest of the T1–T1′ transect (Figure 11). Both shallow and deep

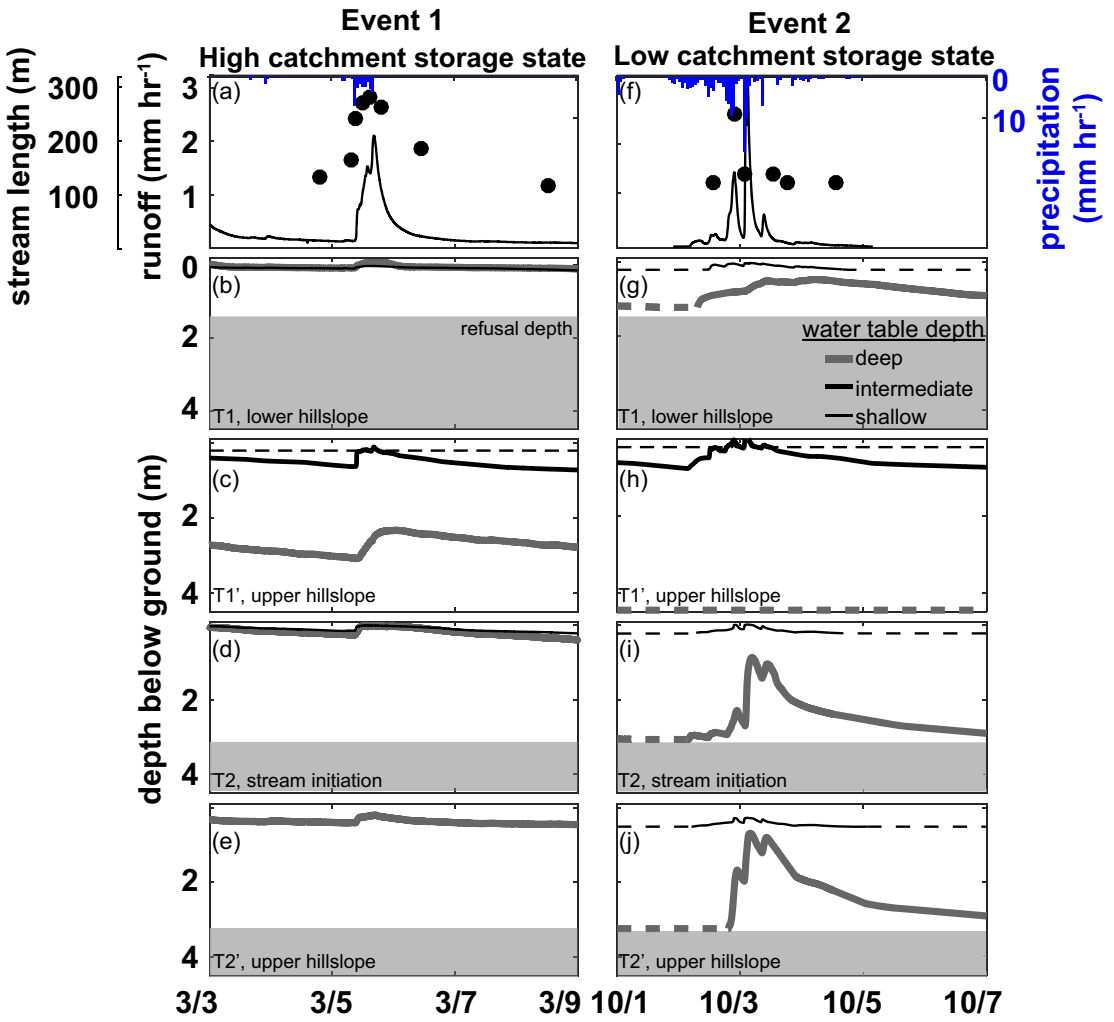

Figure 11. (left column) (a) Runoff (black line), active surface drainage length (black circles), precipitation (blue bars) and (b–e) nested groundwater response during a precipitation event when catchment storage was high (Event 1). (right column) (f) Runoff (black line), active surface drainage length (black circles), precipitation (blue bars) and (g–j) nested groundwater response during a precipitation event when catchment storage was low (Event 2). Dashed line represents when no groundwater was detected at specific well. See Figure 1 for location of groundwater well nests.

water tables responded to the precipitation event but stayed vertically isolated from each other (Figure 11). The water table in the deeper wells at the lower hillslope locations (T1 and T2) responded to precipitation before the perched water table in the shallow wells. In contrast, the perched water table in the shallow well at the upper hillslope well nest (T2′) responded to precipitation before the deeper water table and there was no deep water table response at the upper hillslope (T1′). The shallow and intermediate wells at the upper hillslope nest in T1–T1′ were vertically connected. In all shallow and deep wells in the T2–T2′ transect, groundwater response was flashy and responsive to increases in precipitation intensities (Figure 11). The deeper well in the lower hillslope of T1–T1′ transect had a subdued response to precipitation inputs. Across all nests, the perched shallow water table was only active when the stream was active, while groundwater levels in the deeper wells declined until the next precipitation event, which occurred 5 days after runoff ceased.

4. Discussion

To date, the majority of our understanding of runoff processes has originated from studies that were conducted in steep landscapes with shallow soils. In addition, few studies have linked knowledge about runoff generation processes to the longitudinal expansion of stream networks. We sought to address this by

investigating the runoff generation processes leading to ephemeral and intermittent runoff and surface drainage expansion in a poorly understood, deeply weathered, low relief landscape. We observed process equifinality in that we observed a consistent relationship between active surface drainage length (ASDL) and runoff despite large variability in internal flow path mechanisms, precipitation magnitudes and intensities, and catchment storage states (Figures 6 and 8). Here we discuss and provide explanations, summarized by a conceptual diagram, for the mechanisms driving process equifinality in the generation and characteristics of intermittent and ephemeral runoff.

4.1. Shallow Flow Paths Drive Runoff-Active Surface Drainage Length Relationship

The ability to predict ASDL based on geomorphic or hydrologic parameters is a task researchers have attempted to address for decades [*Carlston*, 1963; *Blyth and Rodda*, 1973; *Dingman*, 1978], due in part to the tremendous ecological significance of these network dynamics [*Stanley et al*., 1997; *Larned et al*., 2010]. To many, streams are conceptualized as a surficial expression of local groundwater [*Winter et al*., 1998; *Bencala et al*., 2011], thus monitoring and predicting ASDL expansion and contraction can also provide insight into subsurface processes [e.g., *Godsey and Kirchner*, 2014; *Shaw*, 2015].

Based on data collected from 77 ASDL mapping campaigns across the study period, we observed that ASDL was nonlinearly correlated to runoff ($r^2 = 0.81$; Figure 5). This ASDL-runoff relationship was not necessarily dependent on catchment storage state, as both low and high catchment storage states were represented across a wide range of ASDLs. As runoff increased from 0 to 0.2 mm h^{-1}, ASDL rapidly increased from 0 to 124 m, which marked the full extent of the geomorphic channel network. Activation of surface flow beyond the geomorphic channel extent and into zero order hollows (>124 m ASDL) was coincident with substantial increases in runoff (Figure 5). Beyond 124 m of ASDL, we observed an increasing rate of runoff per meter of channel extension. We liken this behavior to the transmissivity feedback mechanism of runoff generation seen in shallow soil horizons, where runoff can increase markedly as the water table rises into highly transmissive soil layers [*Bishop*, 1991]. The observed logarithmic relationship with a maximum ASDL suggests that increasing precipitation and widespread shallow subsurface and/or overland flow paths rapidly delivered water to the stream channel leading to increased runoff [*Brown et al*., 1999]. With recent attention focused on the form and function of temporary streams [*Acuña et al*., 2014], these results provide valuable insight into the predictability of temporary stream activation through a commonly measured parameter, runoff. However, we do not yet know if or how this relationship might change with increasing catchment size and we suggest that more work is needed on this topic.

There was scatter in the ASDL-runoff relationship at intermediate ASDL values (~124–268 m), which we attributed to observed counterclockwise hysteresis between ASDL and runoff recorded across individual precipitation events (Figure 5). This counterclockwise event hysteresis only occurred when catchment storage was high; there was no hysteretic pattern when catchment storage was low. We attributed this hysteresis to changes in subsurface flow path contributions across the storm hydrographs. On the rising limb of the stormflow hydrograph, shallow, rapid flow paths were activated, which we showed in two events with contrasting storage states in Figure 11. The shallow flow path contributions were either from shallow, transient, perched water table activation when catchment storage state was low (Event 2) or from the rising of the deeper water table into more transmissive, shallow soil horizons when catchment storage state was high (Event 1). This interpretation is consistent with other studies that have shown that shallow perched water tables in an array of landscapes can deliver water to the stream rapidly at the onset of precipitation events [*Brown et al*., 1999; *Kinner and Stallard*, 2004; *de Moraes et al*., 2006]. On the receding limb of the stormflow hydrographs, the shallow flow path contributions decreased as the water tables dropped. When catchment storage was high, the slower, potentially more spatially expansive deeper water table still contributed to runoff even after shallow flow paths ceased. This caused higher ASDLs on the receding limb of the storm hydrograph. When storage state was low, the deeper water table was not a substantial contributor to runoff (e.g., Figure 11), therefore, there was no hysteretic behavior in the ASDL-runoff relationship when catchment storage was low.

4.2. Event Recession Rates Highlight Shifting Streamflow Contributions With Storage State

Our results highlighted that dominant runoff contributions shift as the catchment storage state shifts. When storage is high, runoff contributions are some combination of both perched, shallow and deep water tables. When storage state is low, runoff contributions are dominated predominantly by shallow,

transient, perched water tables (e.g., Figures 10 and 11). We argued previously that this difference in flow path dominance drove minor hysteresis seen in ASDL-runoff relationships for individual precipitation events, in that the presence of both deeper water table and shallow flow path contributions produced counterclockwise hysteresis (Figure 5). These two water sources contributed different amounts to runoff at disparate times throughout the storm hydrograph, producing this hysteresis pattern. These observations were further supported by sharp differences in hydrograph recession characteristics between precipitation events that occurred across a range of storage states (Figure 7). Results from a hydrograph recession analysis showed consistently faster recession rates when catchment storage was low relative to when storage was high (Figure 7). This is consistent with our interpretation that deeper, slower contributing flow paths were not dominant water sources during drier periods. Instead, shallow flow paths located in more transmissive soil horizons drove stormflow when catchment storage was low. This difference is also evident in the hydrograph recessions of the precipitation events with contrasting catchment storage states highlighted in Figure 11.

4.3. Summary of Mechanisms for Nonperennial Runoff Generation

4.3.1. Climatic Forcing Drives Seasonal Differences in Internal Catchment Runoff Generation Processes

Our results showed that runoff at the catchment outlet was seasonally persistent (i.e., intermittent flow) due to continual contributions from the deeper water table when catchment storage was high (Figures 2 and 9). When catchment storage state was low, ephemeral runoff occurred at the catchment outlet due to transient contributions from a shallow, perched water table activated by precipitation (Figures 2 and 9). While runoff occurred with or without a measureable rise in the deeper water table, shallow flow path activation was consistently coincident with runoff activation (Figure 10). We observed that climatic forcings that mediated evapotranspiration drove these seasonal water table and runoff dynamics.

Shallow soil moisture has been shown to often display either a wet or dry state, with a minimal transitional period bridging the two states [*Grayson et al*., 1997]. This temporal soil moisture pattern can be used as a proxy to represent catchment storage state. At our site, catchment storage state was driven by seasonal evapotranspiration (Figure 2). As a result, the shallow soil moisture, the deeper water table, and the persistence of runoff displayed a pattern that reflected seasonal evapotranspiration (Figures 2 and 9).

When catchment storage state was high, the deep water table rose and contributed substantially to sustain runoff (Figures 9 and 10). During precipitation events, this water table rose further still, entering the upper, more transmissive portions of the soil profile (Figure 11), where rapid lateral subsurface flow could occur. This "transmissivity feedback" mechanism has been demonstrated in several benchmark studies [*Lundin*, 1982; *Bishop*, 1991; *Kendall et al*., 1999]. We believe this mechanism also drove the asymptotic relationship between ASDL and runoff described earlier (Figure 5). Evidence of this mechanism was clear in Event 1 (section 3.4.1; Figure 11), where groundwater responses were coincident in the shallow and deep wells in lower hillslope locations, suggesting no perching occurred. Runoff and groundwater had simultaneous initial responses to precipitation inputs, but water table levels plateaued while runoff continued to increase. This suggested subsurface flow was more rapid in the upper soil horizons due to high K_{sat} values (Figure 4) in accordance with the transmissivity feedback mechanism of stormflow generation.

As catchment storage state decreased, the deep water table declined and eventually ceased contributions to runoff (Figures 9 and 10). During this period, streamflow and groundwater activation were only observed in direct response to precipitation events (Figures 2 and 9). *Zimmer and McGlynn* [2017a] and *Zimmer and McGlynn* [2017b] showed in these periods, when runoff and groundwater were activated, the groundwater gradient was away from the stream, leading to streamflow enhanced groundwater recharge. During these periods, the shallow, transient, perched water table was observed at multiple depths (A/Bt and Bt/C horizon interfaces) in the soil profile across the upper hillslopes in direct response to precipitation (Figure 9). During Event 2 (section 3.4.2), the shallow water table stayed disconnected from the deeper water table in every landscape position (Figure 11). Further, the shallow groundwater dynamics mirrored runoff dynamics, which suggested a tightly coupled system with rapid hillslope contributions to the stream. This was confirmed by the steeper recession characteristics for stormflow hydrographs that occurred when catchment storage state was low (Figure 7). It is clear the interaction of climate induced catchment storage state and subsurface soil structure (Figure 4 and Table 1) played a significant role in these observations.

4.3.2. Soil Characteristics Drive Internal Catchment Runoff Generation Processes

In this study, we observed process equifinality in that the mechanisms producing shallow flow paths varied seasonally, either due to perching when catchment storage was low or to a rise in the deep water table into the shallow, transmissive soil horizons when catchment storage was high. These shallow flow paths had a significant influence on runoff response, independent of catchment storage state. Figure 10 highlighted this relationship for one well nest at an upper hillslope location, however this relationship was consistent across all 12 well nests distributed throughout the catchment. Based on these observed hydrometric responses across the landscape, we determined that shallow flow paths created a hillslope-riparian-stream connection that is relatively common and independent of catchment storage state and deeper groundwater levels. This observation stands in contrast to several studies that have shown connectivity was limited to brief periods when catchment storage state was high [*McGlynn and McDonnell*, 2003; *Jencso et al*., 2009; *Tromp-van Meerveld and McDonnell*, 2006; *Detty and McGuire*, 2010]. In those studies, hillslope-stream connectivity was determined based on the establishment of a water table that originated at or below the soil-bedrock interface. In contrast, in this study the activation of shallow flow paths allowed for hillslope connectivity to occur independent of the presence of the deeper water table.

Development of shallow flow paths was possible due to the soil stratigraphy and structure in this highly weathered landscape (Table 1 and Figure 4). Based on our soil characterization (see section 2.2), we observed abrupt decreases in K_{sat} at soil horizon breaks, specifically at the A/Bt and Bt/C horizon interfaces (Table 1 and Figure 4). These rapid decreases in K_{sat} promoted development of shallow, transient, perched water in response to precipitation events in the lower hillslopes when catchment storage state was low and throughout the year in the upper hillslopes (Figure 9). The development of transient, perched water tables due to vertically nonuniform soil characteristics has been linked to catchment runoff responses in several other studies [*Betson and Marius*, 1969; *Miller et al*., 1971; *Kirkby and Chorley*, 1967; *Scanlon et al*., 2000; *Needelman et al*., 2004; *McDaniel et al*., 2008; *Heller and Kleber*, 2016]. *Elsenbeer* [2001] advanced the concept of hydrologic end members for highly weathered soils by categorizing soil types by whether or not they promote shallow flow path partitioning. Included in this conceptual model were Ultisols, which are the dominant soil order in the Piedmont region of the southeastern U.S. *Elsenbeer* [2001] classified Ultisols as having rapid and laterally focused flow paths due to an increase in clay content and decrease in K_{sat} with depth, which is in alignment with the soil characteristics measurements from our subtropical Piedmont field site. *Elsenbeer* [2001] called for more research in order to connect the presence of shallow flow paths to runoff generation dynamics. Researchers have begun to address this challenge [e.g., *Kinner and Stallard*, 2004; *Crespo et al*., 2011]. For instance, *Johnson et al*. [2006] and *Godsey et al*. [2004] conceptualized hydrologic flow path partitioning in weathered soils by relating and differentiating rapid, transient shallow flow paths from deeper, slower flow paths in tropical landscapes. However, few studies include direct observation of internal processes, especially across contrasting regions, climates, and storage states. To address this, we summarized our results in a conceptual model of temporary (e.g., intermittent and ephemeral) runoff generation mechanisms for low relief landscapes with deep soil. We aimed to not only further conceptualize the hydrologic flow paths in weathered soils, but to extend this conceptualization to include the influences of climate and catchment storage on hydrologic flow paths and to the resulting active surface drainage length and runoff dynamics.

4.4. Conceptual Model of Ephemeral and Intermittent Runoff Generation Mechanisms in a Low Relief, Highly Weathered Landscape

Here we present a conceptual model (Figure 12) in order to summarize the results of our work in the context of the two research questions we sought to address in this study (see section 1). Our results showed that seasonal evapotranspiration produced two dominant catchment storage states, either high (Figure 12a) or low (Figure 12b). Within each storage state, we saw different dominating runoff generation mechanisms that produced process equifinality and distinct runoff characteristics. When catchment storage was high (Figure 12a), flow originated from both shallow and deep sources (Figures 9–11), which produced persistent runoff at the catchment outlet (i.e., intermittent streamflow; Figure 2). *Zimmer and McGlynn* [2017a] and *Zimmer and McGlynn* [2017b] demonstrated stream-groundwater head gradients were consistently toward the stream during this period.

When catchment storage was low (Figure 12b), runoff at the outlet occurred only in direct response to precipitation events (i.e., ephemeral flow; Figure 2). *Zimmer and McGlynn* [2017a] and *Zimmer and McGlynn* [2017b]

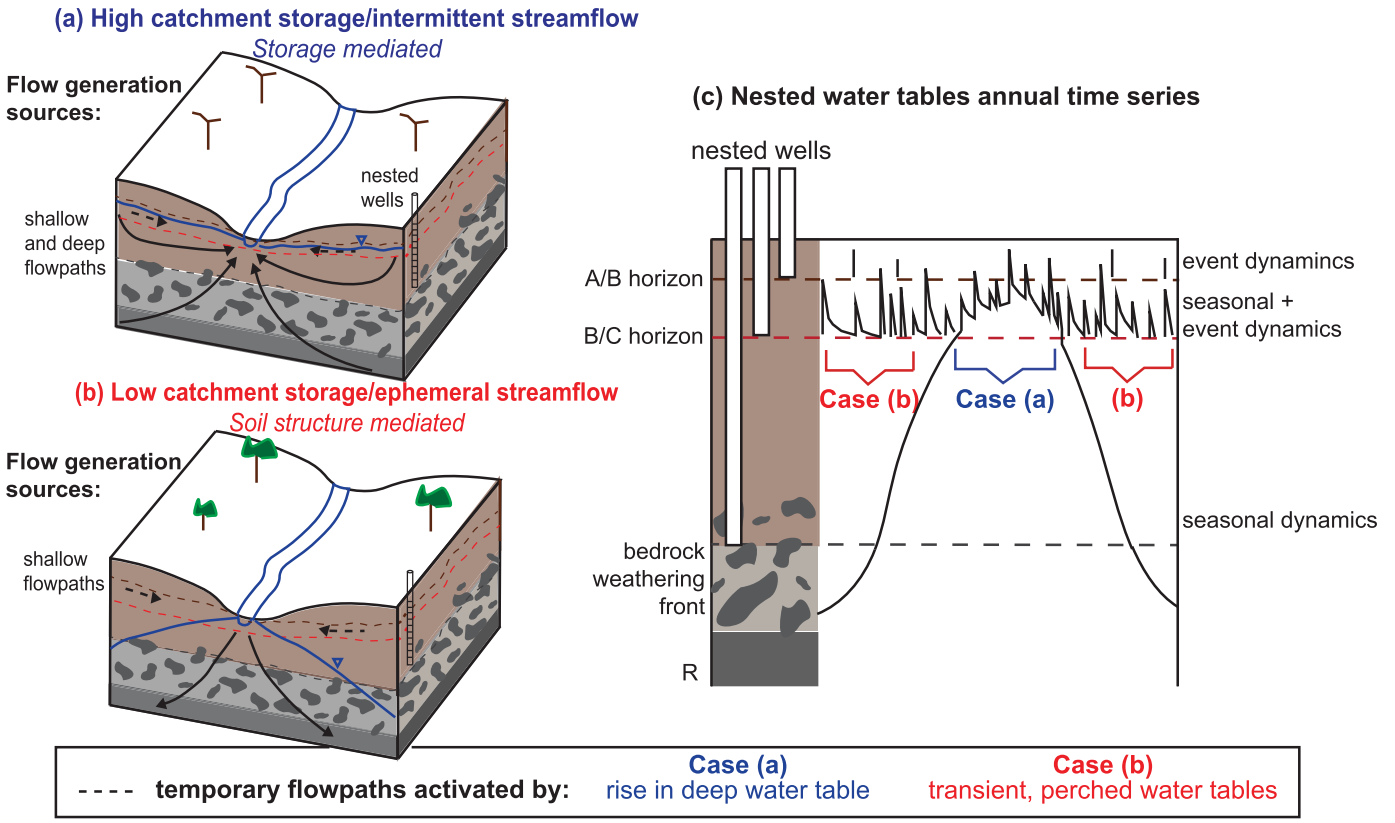

Figure 12. Conceptual model of the runoff generation sources and processes that drive runoff when catchment storage is either high or low. (a) When catchment storage is high, shallow and deep flow paths are contributing to runoff generation through (c) a rise in the deep water table into shallow soil horizons mediated by seasonal soil column storage. During this time, the stream is a gaining system. (b) When catchment storage is low, shallow flow paths contribute to streamflow generation through (c) transient, perched water tables mediated by soil structure. During this time, the stream is losing water to the deeper groundwater system.

demonstrated that stream-groundwater head gradients were consistently away from the stream during this period. Those results suggested an alternative water source apart from the seasonal water table must be generating streamflow. Our results confirmed this hypothesis by showing that runoff was driven by soil structure-mediated perching of transient, shallow water tables (Figures 9–11). With no deep water table contributions to runoff, the activation and magnitude of shallow flow paths depended on the intensity, timing, and magnitude of precipitation events (Figure 9). In either storage state, a strong logarithmic relationship between runoff and active surface drainage length ($r^2 = 0.81$; Figure 5) was driven by activation of shallow flow paths (Figures 11 and 12c).

5. Implications

5.1. Catchment Biogeochemistry Controlled by Internal Catchment Dynamics

From our results, we concluded that shallow flow paths dominated runoff responses and surface drainage network expansion and contraction in this low relief landscape. We believe these results may help inform future runoff generation studies in landscapes with vertically nonuniform soils, resulting either naturally from pedogenesis or from human-induced landscape change. In addition, this new understanding of process equifinality in systems with dominant flow paths driven by soil structure could help explain observed stream biogeochemistry patterns.

Researchers have shown that substantial portions of annual solute export from catchments occur during precipitation events [*Inamdar et al.*, 2004; *Hinton et al.*, 1997; *Creed and Band*, 1998]. This is often due to an increase in the water table height in response to precipitation inputs, which can interact with and flush materials, nutrients, and solutes from a relatively rich pool in shallow soil horizons [*Hornberger et al.*, 1994; *Pacific et al.*, 2010]. In landscapes with steep slopes and thin soils, this shallow flow path activation is

controlled by catchment storage state [e.g., *Lundin*, 1982; *Bishop*, 1991; *Kendall et al*., 1999; *Detty and McGuire*, 2010; *Pacific et al*., 2010]. As a result, large pulses of materials, solutes, and nutrients are often shown to be constrained to seasonally specific events, such as snowmelt, or periods of the year with the highest catchment storage [*Creed and Band*, 1998; *Inamdar et al*., 2004; *Jencso et al*., 2010; *Pacific et al*., 2010; *Pellerin et al*., 2012].

In contrast, our results showed that in this landscape where soil stratigraphy allows for the presence of transient, perched water tables, shallow flow path activation was not necessarily limited by catchment storage state (Figures 9 and 12). In fact, the presence of the deeper water table was not necessary for runoff generation (Figures 5 and 10) and instead, shallow flow path activation was the driving process for increased runoff and active surface drainage expansion. Therefore, while researchers often attribute large solute and nutrient pulses to seasonally specific events, it is possible in landscapes dominated by frequent shallow subsurface flow path activation, such as the Piedmont, near-surface nutrient pools regularly flush from this landscape independent of storage state. Although leaf litter decomposition rates are high in subtropical humid regions such as this landscape, which allows for rapid replenishment of nutrients and solutes at the ground surface [*Meentemeyer*, 1978], it is unclear how frequency of shallow flow path activation influences catchment export of solutes and nutrients. For instance, *Burns et al*. [1998] attributed a higher flushing frequency to greater overall leaching of base cations and thus lower concentrations contributing to the stream. *Boyer et al*. [1997] showed rapid flushing and subsequent depletion of dissolved organic carbon pools from near-surface soil horizons during successive snowmelt pulses. More work is needed to quantify the roles of shallow, transient, perched water tables and deeper, seasonal water tables on nutrient and solute export at the catchment scale.

5.2. Societal Need for a Process-Based Understanding of Temporary Stream Activation

There has been ongoing discussion over the need to lawfully protect temporary streams in the U.S. [*Acuña et al*., 2014; *Alexander*, 2015] due to their important role in biodiversity [*Meyer et al*., 2007] and downstream water quality [*Gomi et al*., 2002]. This has prompted researchers to quantify the extent of these streams, which in turn has highlighted the drastic underestimation of temporary streams in nationally recognized datasets [*Colson et al*., 2008; *Fritz et al*., 2013]. In this study, we highlighted the predominant role of shallow, perched water tables in generation of temporary streams in a Piedmont landscape. It is clear that the conveyance of water through this landscape is highly sensitive to the upper 25 cm of the soil profile. Land use change, such as urbanization or deforestation, may produce unrealized consequences for the mechanisms that delivery water to streams, as these systems are already near the threshold of perched water table development and rapid runoff generation.

Flood mitigation is often cited in arguments for temporary stream protection [*Acuña et al*., 2014]. It is imperative that we understand runoff generation processes in high drainage density landscapes in order to predict how land use change might impact water quantity. We have recorded stream network drainage densities of up to 8.3 km km^{-2} for a 150 ha study catchment associated with this field site, which is in the higher range of recorded drainage densities globally [*Godsey and Kirchner*, 2014], which suggests this region is highly dynamic. However, it is unclear how the pronounced soil stratigraphy of this landscape and resulting erosion and near-surface exposure of low conductivity soil horizons due to land use change might impact these relationships. In addition, the urbanization in the Piedmont region, which comprises much of North Carolina and other eastern states, is expected to increase by 165% over the next 50 years [*Terando et al*., 2014]. Due to the rapid runoff from shallow flow paths and high drainage densities associated with these temporary headwater streams, more work is needed to understand how land use change may impact runoff generation in these and similar systems that are so globally extensive.

6. Conclusions

We linked internal catchment dynamics to surface drainage network expansion and contraction. We characterized dominant hydrologic flow paths in a 3.3 ha catchment draining an ephemeral-to-intermittent drainage network in the nationally expansive Piedmont region of North Carolina, USA. We differentiated the dominant water sources and generation processes by monitoring the timing and magnitude of precipitation, runoff, shallow soil moisture, and shallow and deep groundwater dynamics across characteristic hillslopes for 1.5 years. Through this work, we aimed to not only further conceptualize the hydrologic flow

paths in deeply weathered soils, but also extend this conceptualization to include the influences of climatic forcings and catchment storage on these hydrologic flow paths and to the resulting active surface drainage length and runoff dynamics.

Our results revealed two dominant catchment storage states (high and low) driven by seasonal evapotranspiration. In these two states, distinct subsurface flow paths contributed to runoff and were controlled by the soil structure and stratigraphy characteristic of this highly weathered landscape. The seasonal water table contributed to runoff when catchment storage state was high and the rise and fall of this water table into shallow, more transmissive soil horizons drove runoff dynamics during these periods (Figures 9–12). When catchment storage state was low, activation of shallow, transient, perched water tables dominated runoff (Figures 9–12). High runoff and surface drainage expansion/contraction occurred during both catchment storage states leading to process equifinality at this site.

Despite different groundwater flow path dynamics, the relationship between active surface drainage length (ASDL) and runoff was consistent, independent of catchment storage state (Figure 5). The dependence of runoff on shallow flow path activation across all catchment storage states appeared to drive this relationship (Figure 10). This may suggest shallow flow paths dominate runoff contributions, whereas deeper flow paths have temporally limited importance for runoff, and more work is needed to quantify the contributions of these distinct sources. Evidence of counterclockwise hysteretic behavior between ASDL and runoff for individual precipitation events suggested that while seasonal ASDLs are predicted based on runoff, the generation mechanisms, source waters, and groundwater depths that control flow are highly variable and not easily estimated from runoff dynamics alone. The process equifinality seen internally in this catchment has significant implications for differences in seasonal stream chemistry fluxes from headwaters. We suggest that characterization of internal catchment dynamics can help researchers or practitioners predict flooding, longevity of high or low flows, hydrological impacts of land use change, and associated water quality changes. We suggest that next steps include investigating the hydrological and biogeochemical influence of temporary runoff generation on downstream, perennial watersheds.

Acknowledgments

This study was made possible by Duke University funding to B. L. McGlynn, a National Science Foundation Graduate Research Fellowship to M. A. Zimmer, and funding through the Calhoun Critical Zone Observatory. The authors thank Stephen Architzel, Harley Burton, Mary Tchamkina, Cassandra Harvey, and Ethan Blatt for extensive field work assistance and to Daniel Richter for collaboration and site access to the Duke Forest Research Watershed, a satellite site to the Calhoun Critical Zone Observatory. We also thank Editor D. Scott Mackay and three anonymous reviewers who provided valuable comments on this manuscript. Historical evapotranspiration data can be downloaded at http://ameriflux.lbl.gov. All other hydrometric data can be requested from the corresponding author.

References

Acuña, V., T. Datry, J. Marshall, D. Barceló, C. N. Dahm, A. Ginebreda, G. McGregor, S. Sabater, K. Tockner, and M. A. Palmer (2014), Why should we care about temporary waterways?, *Science*, *343*(6175), 1080–1081.

Alexander, L. C. (2015), Science at the boundaries: Scientific support for the Clean Water Rule, *Freshwater Sci.*, *34*(4), 1588–1594.

Ameli, A. A., J. J. McDonnell, and K. Bishop (2015), The exponential decline in saturated hydraulic conductivity with depth: A novel method for exploring its effect on water flow paths and transit time distribution, *Hydrol. Processes*, *30*, 2438–2450, doi:10.1002/hyp.10777.

Amoozegar, A. (1989), A compact constant-head permeameter for measuring saturated hydraulic conductivity of the vadose zone, *Soil Sci. Soc. Am. J.*, *53*(5), 1356–1361.

Bencala, K. E., M. N. Gooseff, and B. A. Kimball (2011), Rethinking hyporheic flow and transient storage to advance understanding of stream-catchment connections, *Water Resour. Res.*, *47*, W00H03, doi:10.1029/2010WR010066.

Betson, P. B. (1964), What is watershed runoff?, *J. Geophys. Res.*, *69*(8), 1541–1552.

Betson, R., and J. Marius (1969), Source areas of storm runoff, *Water Resour. Res.*, *5*(3), 574–582.

Bishop, K. H. (1991), Episodic increase in stream acidity, catchment flow pathways and hydrograph separation, doctoral dissertation, 246 pp., Univ. of Cambridge, Cambridge, U. K.

Biswal, B., and M. Marani (2010), Geomorphological origin of recession curves, *Geophys. Res. Lett.*, *37*, L24403, doi:10.1029/2010GL045415.

Blyth, K., and J. C. Rodda (1973), A stream length study, *Water Resour. Res.*, *9*(5), 1454–1461.

Bouwer, H., and R. C. Rice (1976), A slug test for determining hydraulic conductivity of unconfined aquifers with completely or partially penetrating wells, *Water Resour. Res.*, *12*(3), 423–428.

Boyer, E. W., G. M. Hornberger, K. E. Bencala, and D. M. McKnight (1997), Response characteristics of DOC flushing in an Alpine Catchment, *Hydrol. Processes*, *11*, 1635–1647.

Bradley, P. J., and N. K. Gay (2005), Geologic map of the Hillsborough 7.5-minute quadrangle, Orange County, North Carolina, in *North Carolina Geological Survey Open-File Rep. 2005 02*, scale 1:24,000, in color, N. C. Geol. Surv., Hillsborough.

Brammer, D. D., and J. J. McDonnell (1996), An evolving perceptual model of hillslope flow at the Maimai catchment, *Adv. Hillslope Process.*, *1*, 35–60.

Brouwer, J., and R. W. Fitzpatrick (2002), Restricting layers, flow paths and correlation between duration of soil saturation and soil morphological features along a hillslope with an altered soil water regime in western Victoria, *Soil Res.*, *40*(6), 927–946.

Brown, V. A., J. J. McDonnell, D. A. Burns, and C. Kendall (1999), The role of event water, a rapid shallow flow component, and catchment size in summer stormflow, *J. Hydrol.*, *217*(3), 171–190.

Brutsaert, W., and J. L. Nieber (1977), Regionalized drought flow hydrographs from a mature glaciated plateau, *Water Resour. Res.*, *13*(3), 637–643.

Burns, D. A., and J. J. McDonnell (1998), Effects of a beaver pond on runoff processes: Comparison of two headwater catchments, *J. Hydrol.*, *205*, 248–264.

Burns, D. A., R. P. Hooper, J. J. McDonnell, J. E. Freer, C. Kendall, and K. Beven (1998), Base cation concentrations in subsurface flow from a forested hillslope: The role of flushing frequency, *Water Resour. Res.*, *34*(12), 3535–3544.

Burt, T. P., and J. J. McDonnell (2015), Whither field hydrology? The need for discovery science and outrageous hydrological hypotheses, *Water Resour. Res.*, *51*, 5919–5928, doi:10.1002/2014WR016839.

Buttle, J. M., and D. J. McDonald (2002), Coupled vertical and lateral preferential flow on a forested slope, *Water Resour. Res.*, *38*(5), doi: 10.1029/2001WR000773.
Carlston, C. W. (1963), *Drainage Density and Streamflow*, U.S. Geological Survey Professional Paper 422-C, pp. 1-8, Washington, D. C.
Chittleborough, D. J. (1992), Formation and pedology of duplex soils, *Aust. J. Exp. Agric.*, *32*(7), 815–825.
Colson, T., J. Gregory, J. Dorney, and P. Russell (2008), Topographic and soil maps do not accurately depict headwater stream networks, *Natl. Wetlands Newsl.*, *30*(3), 25–28.
Cox, J. W., and D. J. McFarlane (1995), The causes of waterlogging in shallow soils and their drainage in southwestern Australia, *J. Hydrol.*, *167*, 175–194, doi:10.1016/0022-1694(94)02614.
Creed, I. F., and L. E. Band (1998), Export of nitrogen from catchments within a temperate forest: Evidence for a unifying mechanism regulated by variable source area dynamics, *Water Resour. Res.*, *34*(11), 3105–3120, doi:10.1029/98WR01924.
Crespo, P. J., J. Feyen, W. Buytart, A. Bücker, L. Breuer, H. G. Frede, and M. Ramírez (2011), Identifying controls of the rainfall-runoff response of small catchments in the tropical Andes (Ecuador), *J. Hydrol.*, *407*, 164–174.
Day, D. G. (1983), Drainage density variability and drainage basin outputs, *J. Hydrol.*, *22*(1), 3–17.
De Moraes, J. M., A. E. Schuler, T. Dunne, R. D. O. Figueiredo, and R. L. Victoria (2006), Water storage and runoff processes in plinthic soils under forest and pasture in eastern Amazonia, *Hydrol. Processes*, *20*(12), 2509–2526.
Detty, J. M., and K. J. McGuire (2010), Topographic controls on shallow groundwater dynamics: Implications of hydrologic connectivity between hillslopes and riparian zones in a till mantled catchment, *Hydrol. Processes*, *24*, 2222–2236, doi:10.1002/hyp.7656.
Devito, K., I. Creed, T. Gan, C. Mendoza, R. Petrone, U. Silins, and B. Smerdon (2005), A framework for broad-scale classification of hydrologic response units on the Boreal Plain: Is topography the last thing to consider?, *Hydrol. Processes*, *19*, 1705–1714, doi:10.1002/hyp.5881.
Dingman, S. L. (1978), Drainage density and streamflow : A closer look, *Water Resour. Res.*, *14*(6), 1183–1187.
Du, E., C. R. Jackson, J. Klaus, J. J. McDonnell, N. A. Griffiths, M. F. Williamson, J. L. Greco, and M. Bitew (2016), Interflow dynamics on a low relief forested hillslope: Lots of fill, little spill, *J. Hydrol.*, doi:10.1016/j.jhydrol.2016.01.039.
Dunne, T., and R. D. Black (1970), Partial area contributions to storm runoff in a Small New England Watershed, *Water Resour. Res.*, *6*(5), 1296–1311.
Elrick, D. E., and W. D. Reynolds (1992), Methods for analyzing constant-head well permeameter data, *Soil Sci. Soc. Am. J.*, *56*(1), 320–323.
Elsenbeer, H. (2001), Hydrologic flowpaths in tropical rainforest soilscapes—A review, *Hydrol. Processes*, *15*(10), 1751–1759.
Fritz, K. M., E. Hagenbuch, E. D'Amico, M. Reif, P. J. Wigington, S. G. Leibowitz, R. L. Comeleo, J. L. Ebersole, and T. L. Nadeau (2013), Comparing the extent and permanence of headwater streams from two field surveys to values from hydrographic databases and maps, *J. Am. Water Resour. Assoc.*, *49*(4), 867–882.
Gannon, J. P., S. W. Bailey, and K. J. McGuire (2014), Organizing groundwater regimes and response thresholds by soils: A framework for understanding runoff generation in a headwater catchment, *Water Resour. Res.*, *50*, 8403–8419, doi:10.1002/2014WR015408.
Godsey, S. E., and J. W. Kirchner (2014), Dynamic, discontinuous stream networks: Hydrologically driven variations in active drainage density, flowing channels, and stream order, *Hydrol. Processes*, *28*, 5791–5803, doi:10.1002/hyp.10310.
Godsey, S. E., H. Elsenbeer, and R. Stallard (2004), Overland flow generation in two lithologically distinct rainforest catchments, *J. Hydrol.*, *295*(1), 276–290.
Gomi, T., R. C. Sidle, and J. S. Richardson (2002), Understanding processes and downstream linkages of headwater systems headwaters differ from downstream reaches by their close coupling to hillslope processes, more temporal and spatial variation, and their need for different means of protection from land use, *BioScience*, *52*(10), 905–916.
Graham, C. B., R. A. Woods, and J. J. McDonnell (2010), Hillslope threshold response to rainfall: (1) A field based forensic approach, *J. Hydrol.*, *393*, 65–76, doi:10.1016/j.jhydrol.2009.12.015.
Grayson, R. B., A. W. Western, F. H. S. Chiew, and G. Blöschl (1997), Preferred states in spatial soil moisture patterns: Local and nonlocal controls, *Water Resour. Res.*, *33*(12), 2897–2908, doi:10.1029/97WR02174.
Hammermeister, D. P., G. F. Kling, and J. A. Vomocil (1982), Perched water tables on hillsides in western Oregon: I. Some factors affecting their development and longevity, *Soil Sci. Soc. Am. J.*, *46*(4), 811–818.
Hardie, M. A., R. B. Doyle, W. E. Cotching, and S. Lisson (2012), Subsurface lateral flow in texture-contrast (duplex) soils and catchments with shallow bedrock, *Appl. Environ. Soil Sci.*, *2012*, 11–16, doi:10.1155/2012/861358.
Heller, K., and A. Kleber (2016), Hillslope runoff generation influenced by layered subsurface in a headwater catchment in Ore Mountains, Germany, *Environ. Earth Sci.*, *75*, 943, doi:10.1007/s12665-016-5750-y.
Hewlett, J. D., and A. R. Hibbert (1963), Moisture and energy conditions within a sloping soil mass during drainage, *J. Geophys. Res.*, *68*(4), 1081–1087, doi:10.1029/JZ068i004p01081.
Hewlett, J. D., and A. R. Hibbert (1966), Factors affecting the response of small watersheds to precipitation in humid areas, *Nat. Sci. Found. Advan. Sci. Semin., Int. Symp. Forest Hydrol. Proc.*, *1965*, 275–290.
Hinton, M. J., S. L. Schiff, and M. C. English (1997), The significance of storms for the concentration and export of dissolved organic carbon from two Precambrian Shield catchments, *Biogeochemistry*, *36*, 67–88, doi:10.1023/A:1005779711821.
Hornberger, G. M., K. E. Bencala, and D. M. McKnight (1994), Hydrological controls on dissolved organic carbon during snowmelt in the Snake River near Montezuma, Colorado, *Biogeochemistry*, *25*, 147–165, doi:10.1007/BF00024390.
Horton, R. E. (1933), The role of infiltration in the hydrologic cycle, *Eos Trans. AGU*, *14*(1), 446–460.
Hursh, C. R. (1936), Storm-water and absorption, *Trans. AGU*, *17*(pt 2), 302.
Inamdar, S. P., S. F. Christopher, and M. J. Mitchell (2004), Export mechanisms for dissolved organic carbon and nitrate during summer storm events in a glaciated forested catchment in New York, USA, *Hydrol. Processes*, *18*, 2651–2661, doi:10.1002/hyp.5572.
Jencso, K. G., and B. L. McGlynn (2011), Hierarchical controls on runoff generation: Topographically driven hydrologic connectivity, geology, and vegetation, *Water Resour. Res.*, *47*, W11527, doi:10.1029/2011WR01066.
Jencso, K. G., B. L. McGlynn, M. N. Gooseff, S. M. Wondzell, K. E. Bencala, and L. Marshall (2009), Hydrologic connectivity between landscapes and streams: Transferring reach- and plot-scale understanding to the catchment scale, *Water Resour. Res.*, *45*, W04428, doi: 10.1029/2008WR007225.
Jencso, K. J., B. L. McGlynn, M. N. Gooseff, K. E. Bencala, and S. M. Wondzell (2010), Hillslope hydrologic connectivity controls riparian groundwater turnover: Implications of catchment structure for riparian buffering and stream water sources, *Water Resour. Res.*, *46*, W10524, doi:10.1029/2009WR008818.
Johnson, A. I. (1963), A Field Method for Measurement of Infiltration, Water Supply Paper 1544-F, U.S. Geological Survey, Reston, Va.
Johnson, M. S., J. Lehmann, E. G. Couto, J. P. Novaes Filho, and S. J. Riha (2006), DOC and DIC in flowpaths of Amazonian headwater catchments with hydrologically contrasting soils, *Biogeochemistry*, *81*(1), 45–57.
Kendall, K. A., J. B. Shanley, and J. J. McDonnell (1999), A hydrometric and geochemical approach to test the transmissivity feedback hypothesis during snowmelt, *J. Hydrol.*, *219*, 188–205, doi:10.1016/S0022-1694(99)00059-1.

Kinner, D. A., and R. F. Stallard (2004), Identifying storm flow pathways in a rainforest catchment using hydrological and geochemical modelling, *Hydrol. Processes*, *18*(15), 2851–2875.
Kirkby, M. J., and R.J. Chorley (1967), Throughflow, overland flow and erosion, *Int. Assoc. Sci. Hydrol. Bull.*, *12*, 5–21, doi:10.1080/02626666709493533.
Larned, S. T., T. Datry, D. B. Arscott, and K. Tockner (2010), Emerging concepts in temporary-river ecology, *Freshwater Biol.*, *55*, 717–738, doi:10.1111/j.1365-2427.2009.02322.x.
Lundin, L. (1982), Soil moisture and ground water in till soil and the significance of soil type for runoff, *UNGI Rep. 56*, 216 pp., Uppsala Univ., Uppsala, Sweden.
McDaniel, P. A., M. P. Regan, E. Brooks, J. Boll, S. Barndt, A. Falen, S. K. Young, and J. E. Hammel (2008), Linking fragipans, perched water tables, and catchment-scale hydrological processes, *Catena*, *73*, 166–173, doi:10.1016/j.catena.2007.05.011.
McGlynn, B. L., and J. J. McDonnell (2003), Quantifying the relative contributions of riparian and hillslope zones to catchment runoff, *Water Resour. Res.*, *39*(11), 1310, doi:10.1029/2003WR002091.
Meentemeyer, V. (1978), Macroclimate and lignin control of litter decomposition rates, *Ecology 59*(3), 465–472.
Meyer, J. L., J. B. Strayer, J. B. Wallace, S. L. Eggert, G. S. Helfman, and N. E. Leonard (2007), The contribution of headwater streams to biodiversity in river networks, *J. Am. Water Resour. Assoc.*, *43*, 86–103.
Miller, F. P., N. Holowaychuk, and L. P. Wilding (1971), Canfield silt loam, a Fragiudalf: I. Macromorphological, physical, and chemical properties, *Soil Sci. Soc. Am. J.*, *35*(2), 319–324.
Montgomery, D. R., and W. E. Dietrich (1988), Where do channels begin?, *Nature*, *336*, 232–234, doi:10.1038/336232a0.
Needelman, B. A., W. J. Gburek, G. W. Petersen, A. N. Sharpley, and P. J. Kleinman (2004), Surface runoff along two agricultural hillslopes with contrasting soils, *Soil Sci. Soc. Am. J.*, *68*, 914, doi:10.2136/sssaj2004.0914.
Novick, K., C. Oishi, and P. Stoy (2016), AmeriFlux US-Dk2 Duke Forest-hardwoods. AmeriFlux; Indiana University; Montana State University; USDA Forest Service, doi:10.17190/AMF/1246047.
Ocampo, C. J., M. Sivapalan, and C. Oldham (2006), Hydrological connectivity of upland-riparian zones in agricultural catchments: Implications for runoff generation and nitrate transport, *J. Hydrol.*, *331*, 643–658, doi:10.1016/j.jhydrol.2006.06.010.
Oishi, A. C., R. Oren, and P. C. Stoy (2008), Estimating components of forest evapotranspiration: A footprint approach for scaling sap flux measurements, *Agric. For. Meteorol.*, *148*, 1719–1732, doi:10.1016/j.agrformet.2008.06.013.
Oren, R., B. E. Ewers, P. Todd, N. Phillips, and G. G. Katul (1998), Water balance delineates the soil layer in which moisture affects canopy conductance, *Ecol. Appl.*, *8*(4), 990–1002.
Pacific, V., K. Jencso, and B. L. McGlynn (2010), Variable flushing mechanisms and landscape structure control stream DOC export during snowmelt in a set of nested catchments, *Biogeochemistry*, *99*, 193–211, doi:10.1007/s10533-009-9401-1.
Pearce, A. J., M. K. Stewart, and M. G. Sklash (1986), Storm runoff generation in humid headwater catchments: 1. Where does the water come from?, *Water Resour. Res.*, *22*(8), 1263–1272, doi:10.1029/WR022i008p01263.
Pellerin, B. A., J. Franco, S. James, and B. A. Bergamaschi (2012), Taking the pulse of snowmelt: In situ sensors reveal seasonal, event and diurnal patterns of nitrate and dissolved organic matter variability in an upland forest stream, *Biogeochemistry*, *108*, 183–198, doi:10.1007/s10533-011-9589-8.
Penna, D., H. J. Tromp-Van Meerveld, A. Gobbi, M. Borga, and G. Dalla Fontana (2011), The influence of soil moisture on threshold runoff generation processes in an alpine headwater catchment, *Hydrol. Earth Syst. Sci.*, *15*, 689–702, doi:10.5194/hess-15-689-2011.
Ragan, R. M. (1968), An experimental investigation of partial area contribution, *Int. Assoc. Sci. Hydrol. Publ.*, *76*, 241–249.
Richter, D. D., D. Markewitz, S. E. Trumbore, and C. G. Wells (1999), Rapid accumulation and turnover of soil carbon in a re-establishing forest, *Nature*, *400*, 56–58, doi:10.1038/21867.
Roberts, M. C., and O. W. Archibold (1978), Variation of drainage density in a small British Columbia watershed, *Water Resour. Bull.*, *14*(2), 470–476.
Roberts, M., and P. Klingeman (1972), The relationship between drainage net fluctuation and discharge, International Geography, Proceedings of the 22nd International Geographical Congress, Canada, Adams and Helleiner (eds.), University of Toronto Press, 189–191.
Rodhe, A., and J. Seibert (2011), Groundwater dynamics in a till hillslope: Flow directions, gradients and delay, *Hydrol. Processes*, *25*, 1899–1909, doi:10.1002/hyp.7946.
Scanlon, T. M., J. P. Raffensperger, G. M. Hornberger, and R. B. Clapp (2000), Shallow subsurface storm flow in a forested headwater catchment: Observations and modeling using a modified TOPMODEL, *Water Resour. Res.*, *36*(9), 2575–2586.
Shaw, S. B. (2015), Investigating the linkage between streamflow recession rates and channel network contraction in a mesoscale catchment in New York state, *Hydrol. Processes*, *30*, 479–492, doi:10.1002/hyp.10626.
Shaw, S. B., T. M. McHardy, and S. J. Riha (2013), Evaluating the influence of watershed moisture storage on variations in base flow recession rates during prolonged rain-free periods in medium-sized catchments in New York and Illinois, USA, *Water Resour. Res.*, *49*, 6022–6028, doi:10.1002/wrcr.20507.
Sidle, R. C., Y. Tsuboyama, S. Noguchi, I. Hosoda, M. Fujieda, and T. Shimizu (1995), Seasonal hydrologic response at various spatial scales in a small forested catchment, Hitachi Ohta, Japan, *J. Hydrol.*, *168*, 227–250, doi:10.1016/0022-1694(94)02639-S.
Sidle, R. C., Y. Tsuboyama, S. Noguchi, I. Hosoda, M. Fujieda, and T. Shimizu (2000), Stormflow generation in steep forested headwaters: A linked hydrogeomorphic paradigm, *Hydrol. Processes*, *14*, 369–385.
Sklash, M. G., M. K. Stewart, and A. J. Pearce (1986), Storm runoff generation in humid headwater catchments: 2. A case study of hillslope and low-order stream response, *Water Resour. Res.*, *22*(8), 1273–1282, doi:10.1029/WR022i008p01273.
Smettem, K. R. J., D. J. Chittleborough, B. G. Richards, and F. W. Leaney (1991), The influence of macropores on runoff generation from a hillslope soil with a contrasting textural class, *J. Hydrol.*, *122*, 235–251.
Soil Survey Staff Natural Resources Conservation Service, United States Department of Agriculture (2016), *Web Soil Survey*. [Available at http://websoilsurvey.nrcs.usda.gov/.]
Spence, C., and S. Mengistu (2016), Deployment of an unmanned aerial system to assist in mapping an intermittent stream, *Hydrol. Processes*, *30*, 493–500, doi:10.1002/hyp.10597.
St Clair, J., S. Moon, W. S. Holbrook, J. T. Perron, C. S. Riebe, S. J. Martel, B. Carr, C. Harman, K. Singha, and D. D. Richter (2015), Geophysical imaging reveals topographic stress control of bedrock weathering, *Science*, *350*, 534–538, doi:10.1126/science.aab2210.
Stanley, E. H., S. G. Fisher, and N. B. Grimm (1997), Ecosystem expansion and contraction in streams dramatically in size, *BioScience*, *47*(7), 427–435.
Terando, A. J., J. Constanza, C. Belyea, R. R. Dunne, A. McKerrow, and J. A. Collazo (2014), The southern megalopolis: Using the past to predict the future of urban sprawl in the Southeast US, *PLoS ONE*, *9*(7), e102261, doi:10.1371/journal.pone.0102261.
Tromp-van Meerveld, H. J., and J. J. McDonnell (2006), Threshold relations in subsurface stormflow: 1. A 147 storm analysis of the Panola hillslope, *Water Resour. Res.*, *42*, W02410, doi:10.1029/2004WR003778.

Tromp-van Meerveld, I. T., and M. Weiler (2008), Hillslope dynamics modeled with increasing complexity, *J. Hydrol.*, *361*, 24–40, doi: 10.1016/j.jhydrol.2008.07.019.
Tsukamoto, Y. (1963), Storm discharge from an experimental watershed, *J. Jpn. For. Soc.*, *45*, 186–190.
U.S. Department of Agriculture (1972), Field Manual for Research in Agricultural Hydrology, Agriculture Handbook No. 224, Washington, D.C.
van Verseveld, W. J., J. J. McDonnell, and K. Lajtha (2008), A mechanistic assessment of nutrient flushing at the catchment scale, *J. Hydrol.*, *358*, 268–287, doi:10.1016/j.jhydrol.2008.06.009.
ven Chow, T. (1964), Runoff, in *Handbook of Applied Hydrology*, edited by T. ven Chow, McGraw-Hill, New York.
Western, A. W., and R. B. Grayson (1998), The Tarrawarra data set: Soil moisture patterns, soil characteristics, and hydrological flux measurements, *Water Resour. Res.*, *34*(10), 2765–2768.
Western, A. W., R. B. Grayson, G. Blöschl, G. R. Willgoose, and T. A. McMahon (1999), Observed spatial organization of soil moisture and its relation to terrain indices, *Water Resour. Res.*, *35*(3), 797–810.
Weyman, D. R. (1970), Throughflow on hillslopes and its relation to the stream hydrograph, *Int. Assoc. Sci. Hydrol. Bull.*, *15*, 25–33, doi: 10.1080/02626667009493969.
Weyman, D. R. (1973), Measurements of the downslope flow of water in a soil, *J. Hydrol.*, *20*, 267–288, doi:10.1016/0022-1694(73)90065-6.
Whiting, J. A., and S. E. Godsey (2016), Discontinuous headwater stream networks with stable flowheads, Salmon River basin, Idaho, *Hydrol. Processes*, *30*, 2305–2316, doi:10.1002/hyp.10790.
Winter, T. C., J. W. Harvey, O. L. Franke, and W. M. Alley (1998), Ground water and surface water: A single resource, *U.S. Geol. Surv. Circ.*, *1139*, 16.
Woods, R., and L. Rowe (1996), The changing spatial variability of subsurface flow across a hillside, *J. Hydrol. N. Z.*, *35*(1), 51–86.
Zimmer, M. A., and B. L. McGlynn (2017a), Time-lapse animation of hillslope groundwater dynamics details event-based and seasonal bidirectional stream-groundwater gradients, *Hydrol. Processes*, doi:10.1002/hyp.11124, in press.
Zimmer, M. A., and B. L. McGlynn (2017b), Bidirectional stream-groundwater flow in response to ephemeral and intermittent streamflow and groundwater seasonality, *Hydrol. Processes*, doi:10.1002/hyp.11301, in press.